Multi-wavelength, long-term behavior of LS I +61 303

Changes of state in a flip-flopping gamma-ray binary system

Diego F. Torres

*Research done in collaboration with **D. Hadasch**, J. Li, N. Rea, A. Papitto, et al.*

Research done with the support of

*iCrea INSTITUCIÓ CATALANA DE RECERCA I ESTUDIS AVANÇATS

IEEC INSTITUT D'ESTUDIS ESPACIALS DE CATALUNYA

CSIC CONSEJO SUPERIOR DE INVESTIGACIONES CIENTÍFICAS

Main parameters of LS I +61 303

- Compact object + Be star
  - Be stars: B-type stars that lose mass in an equatorial, circumstellar disk

- Orbital period
  - (**26.496** +/- 0.0028 days) (Gregory et al. 2002)
  - e = 0.5-0.7
  - d = 2.0 +/- 0.2 kpc

- Superobital period (Gregory et al. 2002)
  - (**1667** +/- 8) days
  - First seen in radio

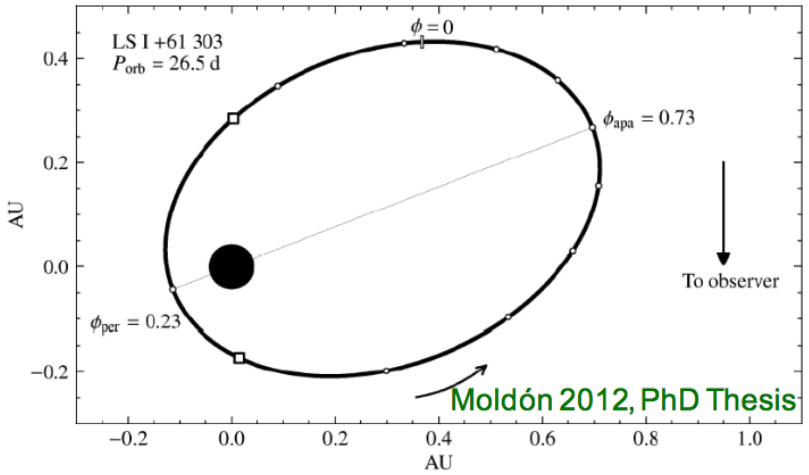

Plot from Chernyakova et al. 2006

LS I +61 303 is a TeV variable source, with orbital phenomenology

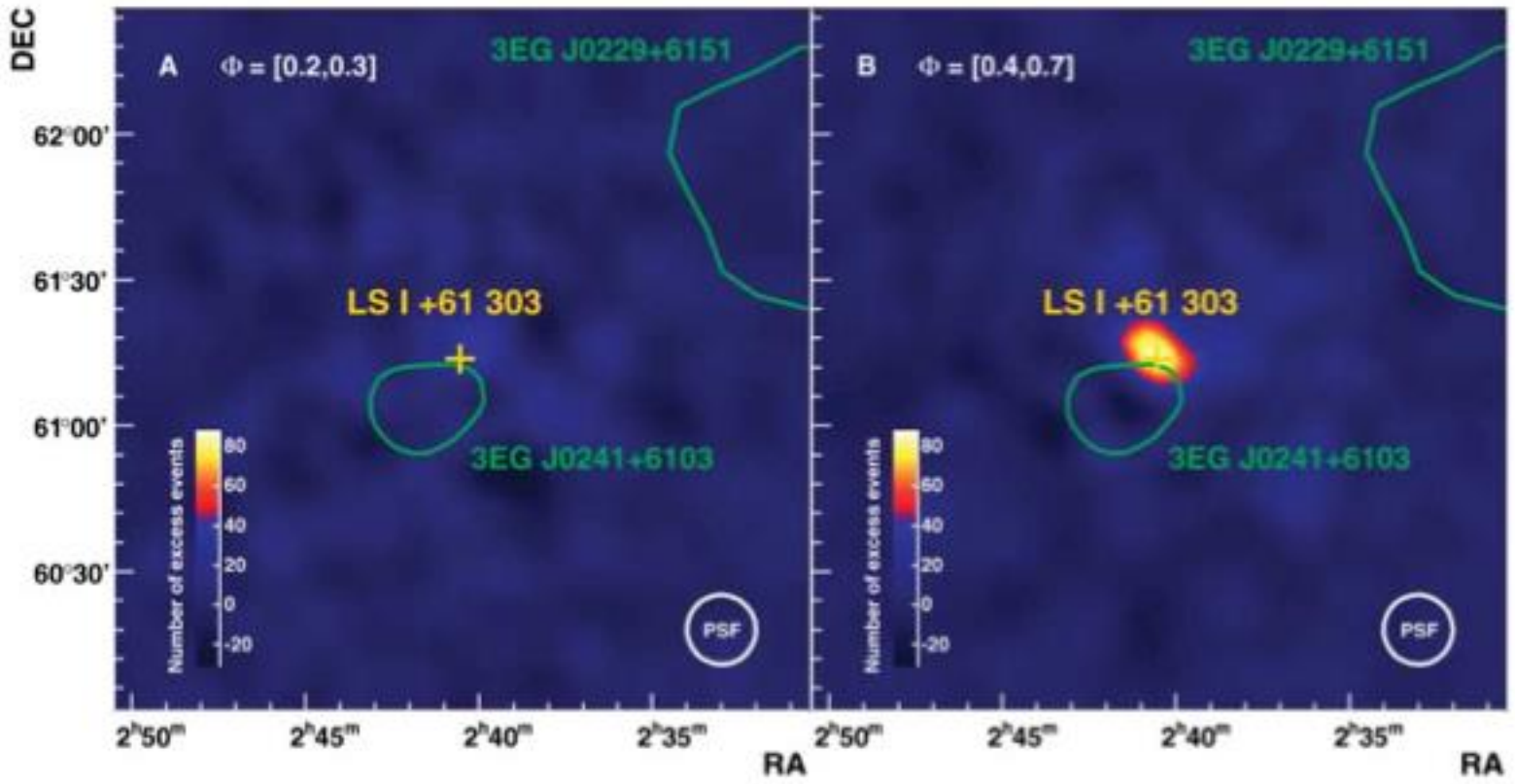

Plots from MAGIC collaboration (2006), published in Science.

Before Fermi, no confirmed GeV binaries

LS 5039

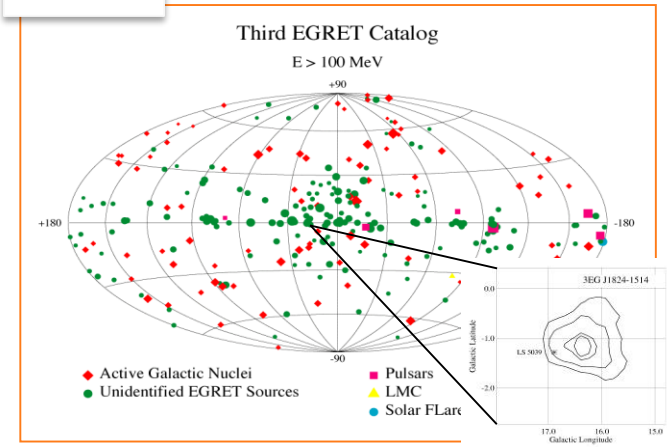

Paredes et al. 2000

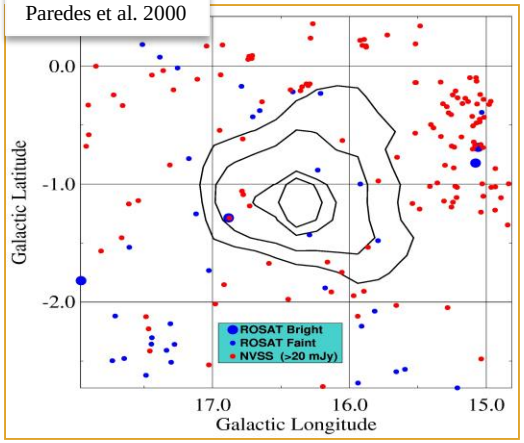

Paredes et al. 2000

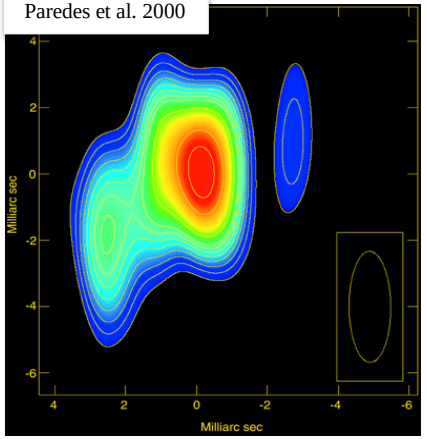

30/9/76 Hermsen

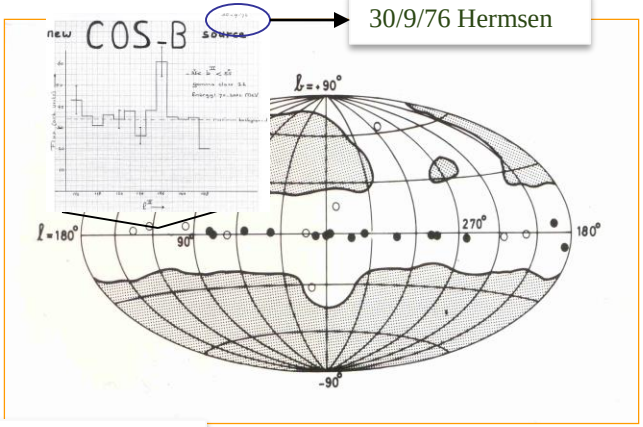

LS I +61 303

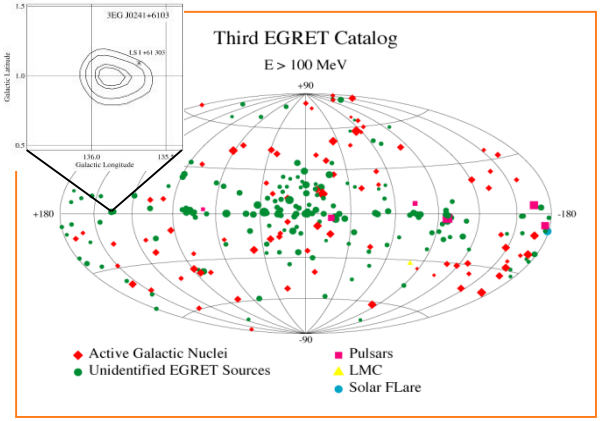

No confirmed (orbital) variability // Bad positioning // many candidates in the field led these sources to remain unidentified

e.g., Torres et al. 2001, A&A; Torres et al. 2003 Physics Reports

Early GeV confirmation of orbital variability, with Fermi-LAT

THE ASTROPHYSICAL JOURNAL, 701:L123–L128, 2009 August 20 doi:10.1088/0004-637X/701/2/L123

FERMI LAT OBSERVATIONS OF LS I +61°303: FIRST DETECTION OF AN ORBITAL MODULATION IN GeV GAMMA RAYS

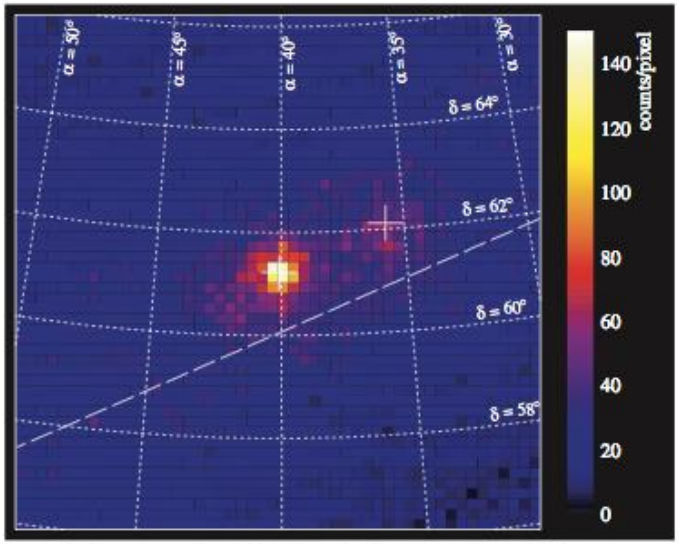

Figure 1. Counts map for 100 MeV–300 GeV in (R.A., decl.) of a 10° region around the LS I +61°303 location. The exposure varies by less than 2.5% across the field at a representative energy of 10 GeV. The source is bright and fairly isolated, sitting on a background of Galactic and extragalactic diffuse emission. A fit to the source yields a significance of more than 70σ. The dashed line indicates the Galactic equator ($b = 0$); the crosses indicate the location of LS I +61°303 (the brighter source) and a faint nearby point source.

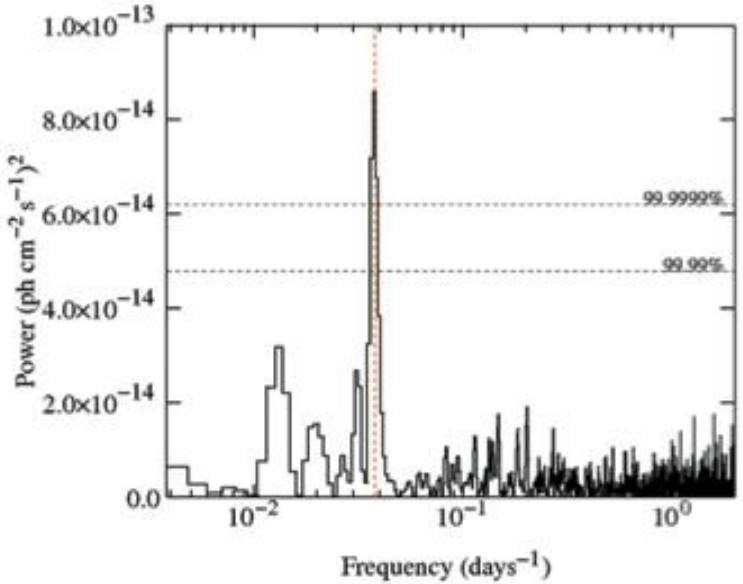

Figure 4. Power spectrum of the light curve. The vertical line indicates the known orbital period from Gregory (2002), coinciding with a strong peak in the spectrum, while the horizontal lines indicate the marked significance levels.

Plots from Abdo et al. 2009 (RD, AH, DFT as corresponding

Dichotomy in composition: discussion in the literature

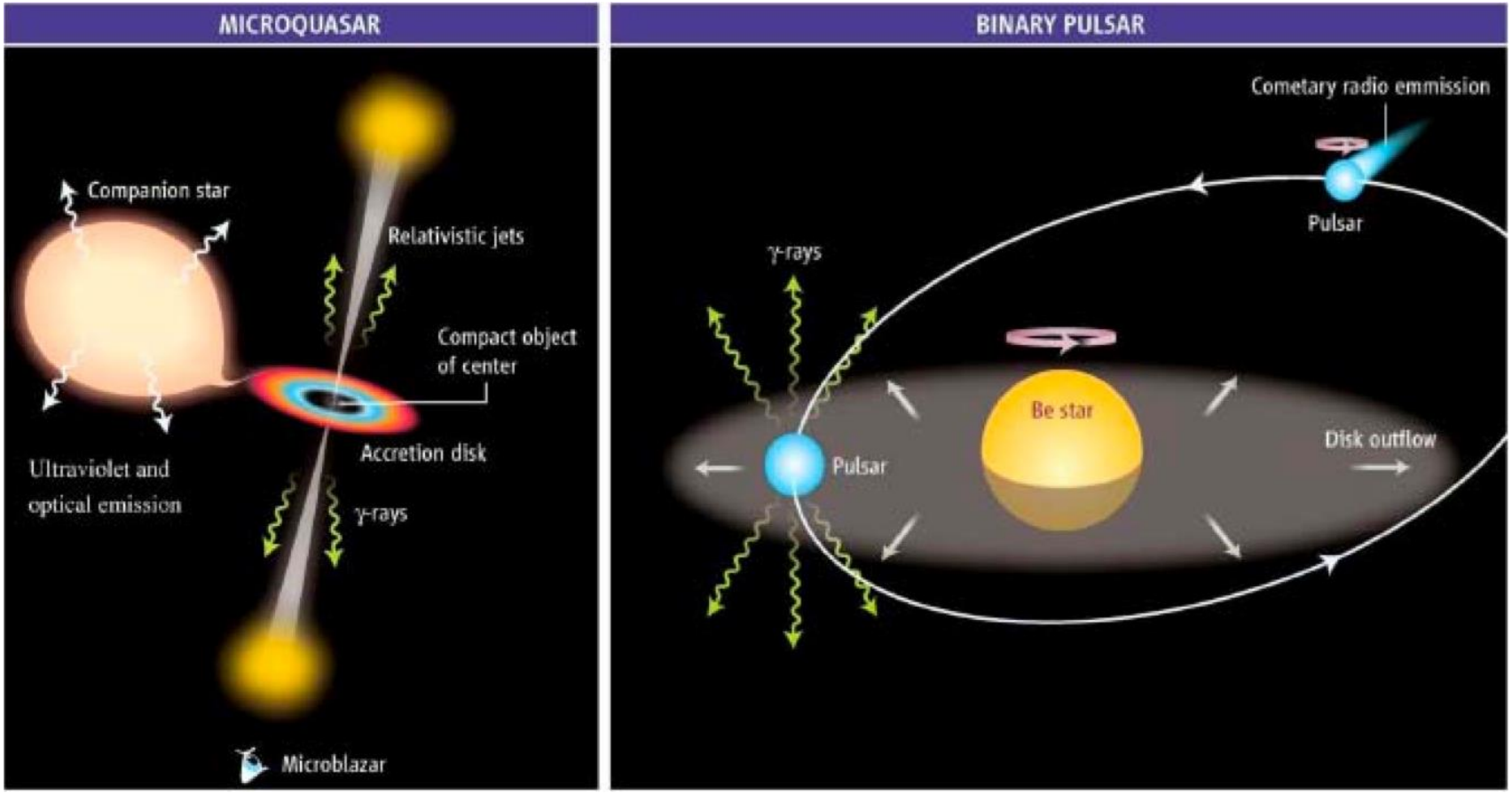

Plot from Mirabel 2006

But the reality is more complicated than this

-Short timescale phenomenology essentially at all frequencies with properties
-… beyond simplifying assumptions of both models.

-Among that, bursts with timescales of less than a a second detected
-…twice from LS I 61 303

-Clear TeV phenomenology at longer timescales showing low and high-states
-… with broad distribution of TeV detection around apastron in orbital scales

Magnetar-like flares

Burst duration is typical of magnetar-like bursts (0.01–1 s)

Burst spectra consistent with magnetar bursts, in particular similar of those observed from AXPs (kT~6–10 keV) which are slightly softer than SGR–like one

The burst flux at 2 kpc implies a 15–50keV luminosity of ~ few × 10^{37} erg s^{-1} , in line with AXP values, which are usually slightly less powerful than SGR ones.

Burst flux much beyond X-ray luminosity of the system

1st detected short-timescale X-ray burst in LS I 61 303: Sept. 2008

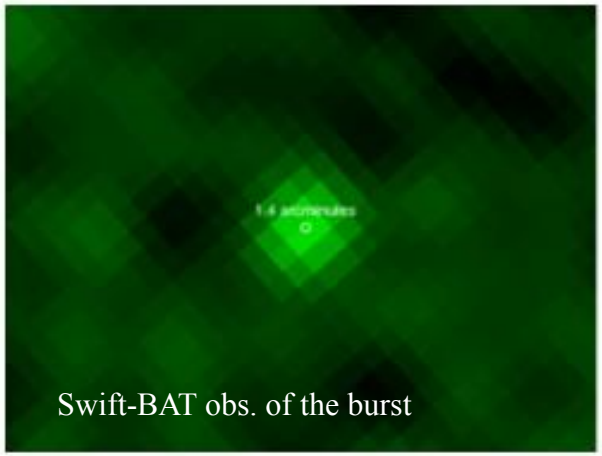

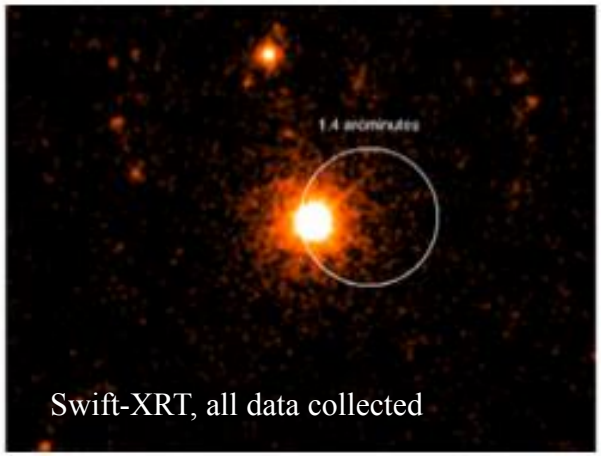

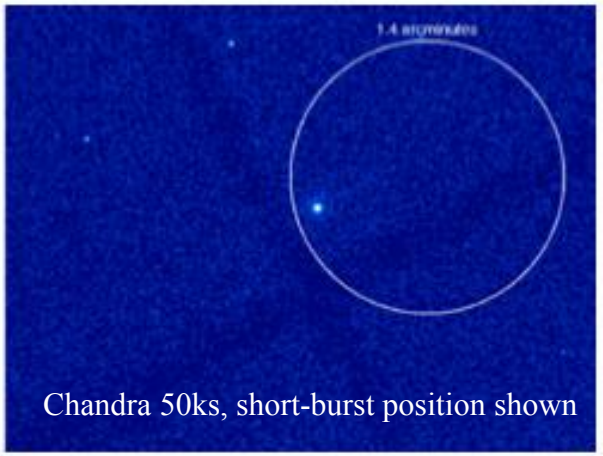

Figure 3. From left to right: the *Swift*/BAT image of the short burst (see Section 2.1) superimposing the spatial accuracy of our position determination (1.′4); the *Swift*–XRT image of all of the data collected so far on LS I +61°303 (165 ks), with the 1.′4 *Swift*/BAT error circle superimposed; and the *Chandra*/ACIS 50 ks image of the field of LS I +61°303 with the short burst positional accuracy overimposed.

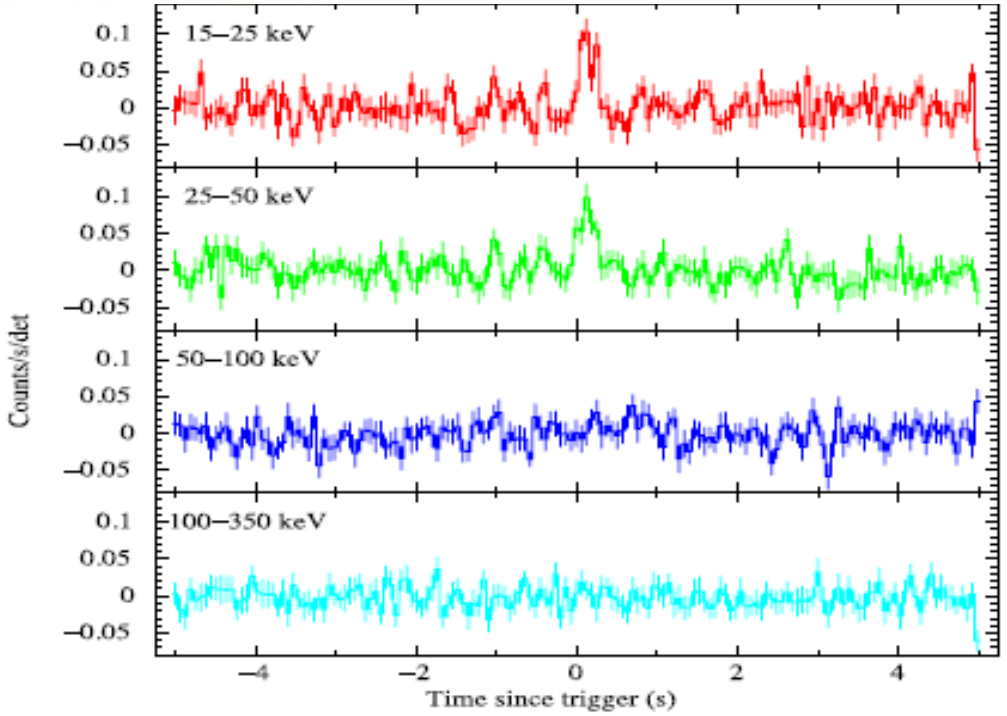

Plot from Torres et al. 2012, ApJ

TeV emission has a high and low state: MAGIC low-detection

DETECTION OF THE γ-RAY BINARY LS I +61°303 IN A LOW-FLUX STATE AT VERY HIGH ENERGY γ-RAYS WITH THE MAGIC TELESCOPES IN 2009

We present very high energy ($E > 100$ GeV) γ-ray observations of the γ-ray binary system LS I +61°303 obtained with the MAGIC stereo system between 2009 October and 2010 January. We detect a 6.3σ γ-ray signal above 400 GeV in the combined data set. The integral flux above an energy of 300 GeV is $F(E > 300\,\mathrm{GeV}) = (1.4 \pm 0.3_{\mathrm{stat}} \pm 0.4_{\mathrm{syst}}) \times 10^{-12}\,\mathrm{cm}^{-2}\,\mathrm{s}^{-1}$, which corresponds to about 1.3% of the Crab Nebula flux in the same energy range. The orbit-averaged flux of LS I +61°303 in the orbital phase interval 0.6–0.7, where a maximum of the TeV flux is expected, is lower by almost an order of magnitude compared to our previous measurements between 2005 September and 2008 January. This provides evidence for a new low-flux state in LS I +61°303. We find that the change to the low-flux state cannot be solely explained by an increase of photon–photon absorption around the compact star.

About an order of magnitude less luminous in TeV energies than what it emitted a couple of years ago

from Aleksic et al. 2012 (MAGIC collaboration)

Fermi

- Two Fermi instruments:
- **LAT:**

  high energy (20 MeV – 100 GeV)

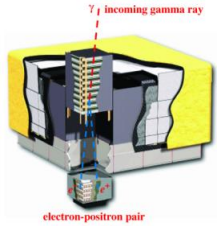

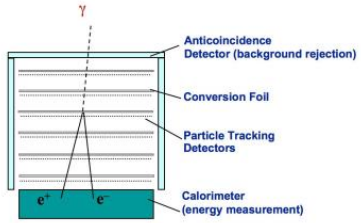

- GBM:

  low energy

  (8 keV – 30 MeV)

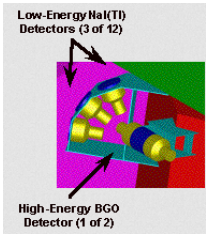

Compared to its predecessor (EGRET):
- > 100 MeV, 1 yr sensitivity x25
- localization x10^2
- field of view x5
- observing efficiency x2
- deadtime x10^{-3}

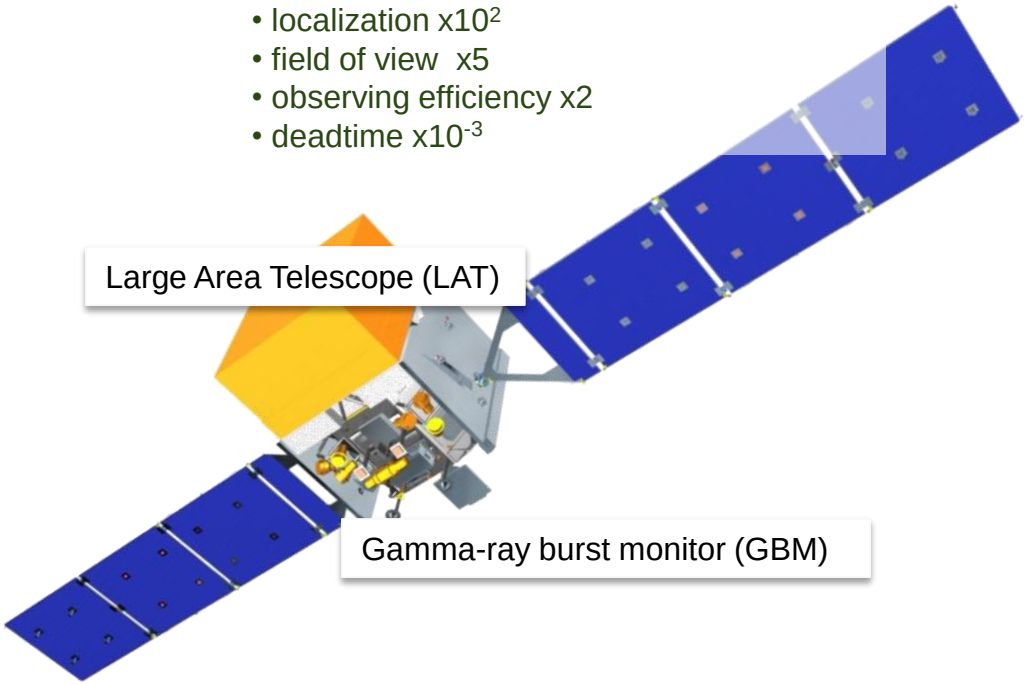

- Huge field of view
  - LAT: 20% of the sky at any instant; in sky survey mode, expose all parts of sky for ~30 minutes every 3 hours. GBM: whole unocculted sky at any time.
  - Large energy range, including largely unexplored band 10 GeV - 100 GeV

- The PI is P. Michelson (SLAC & Stanford), leading a constructing consortium of 5 nations and a scientific consortium of 13 (including Spain)

GeV flux evolution

Ackermann et al. 2013 (D. Hadasch, A. Caliandro, J. Li, and DFT corresp. authors)

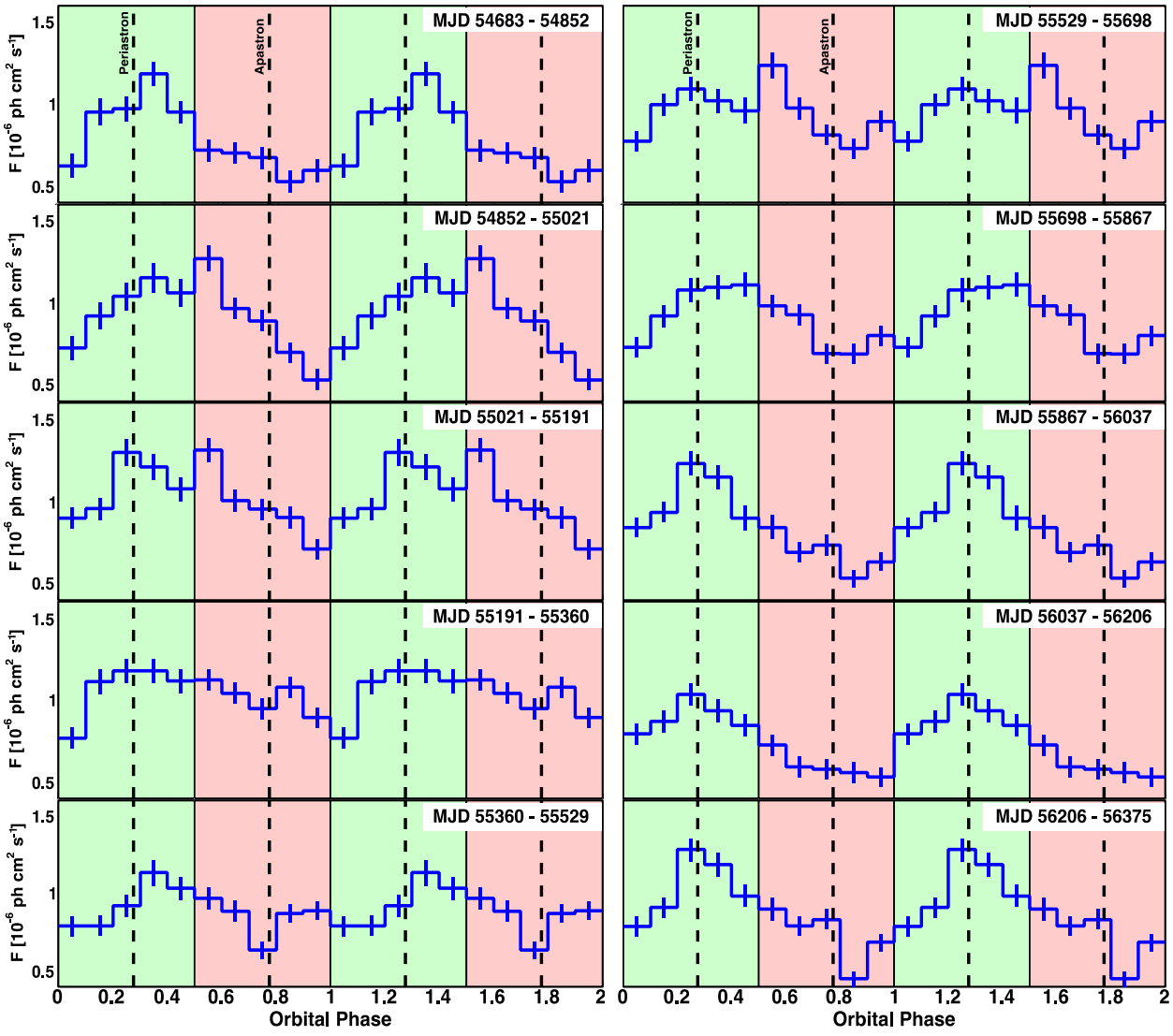

Each panel is ~6 months integration of Fermi data.

The background represents regions of **periastron** and **apastron**, respectively

Trends for location of max and min, visible

Maximum near periastron, but with significant variability

Variability of lightcurve along the orbital phases

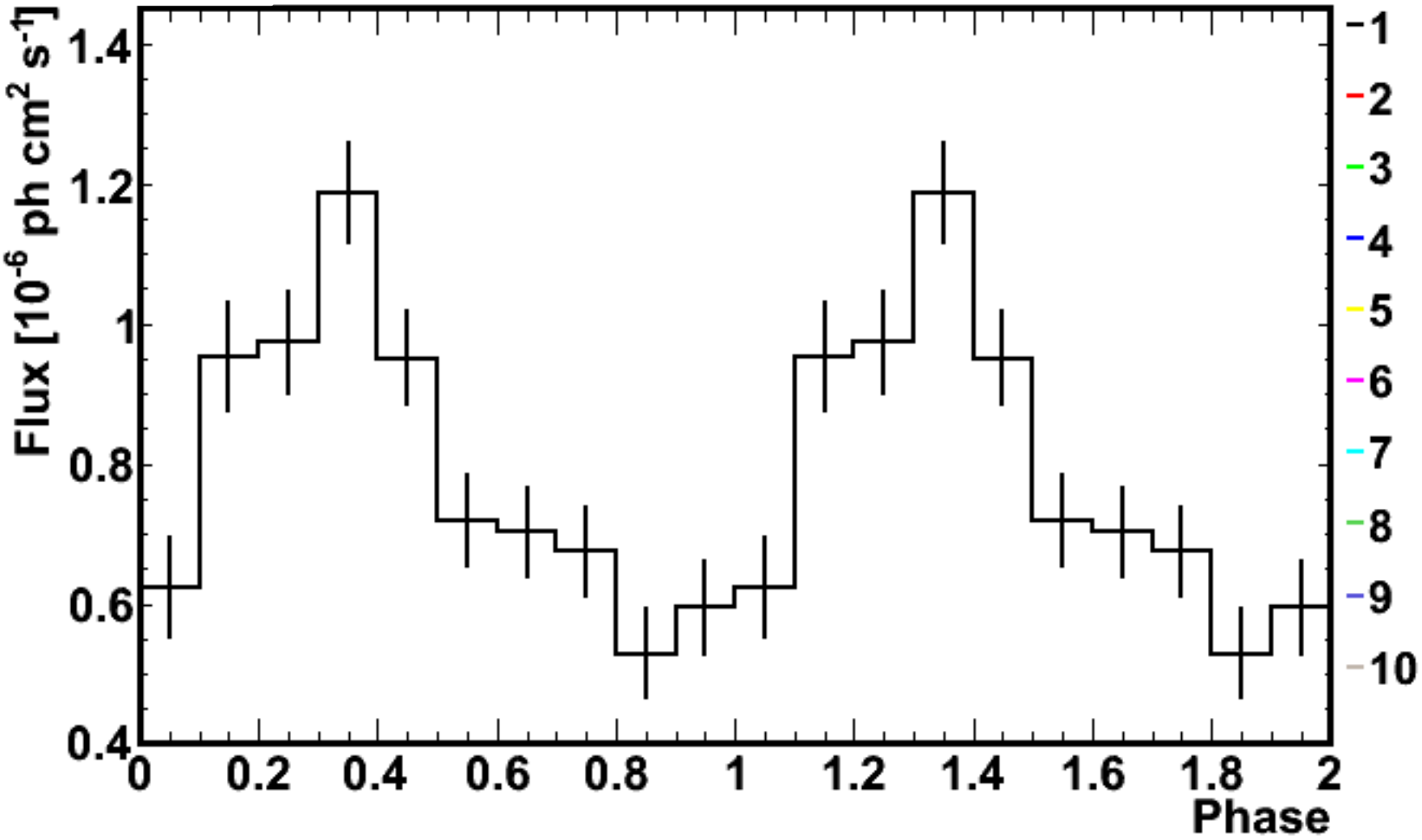

GeV flux evolution along the superorbit

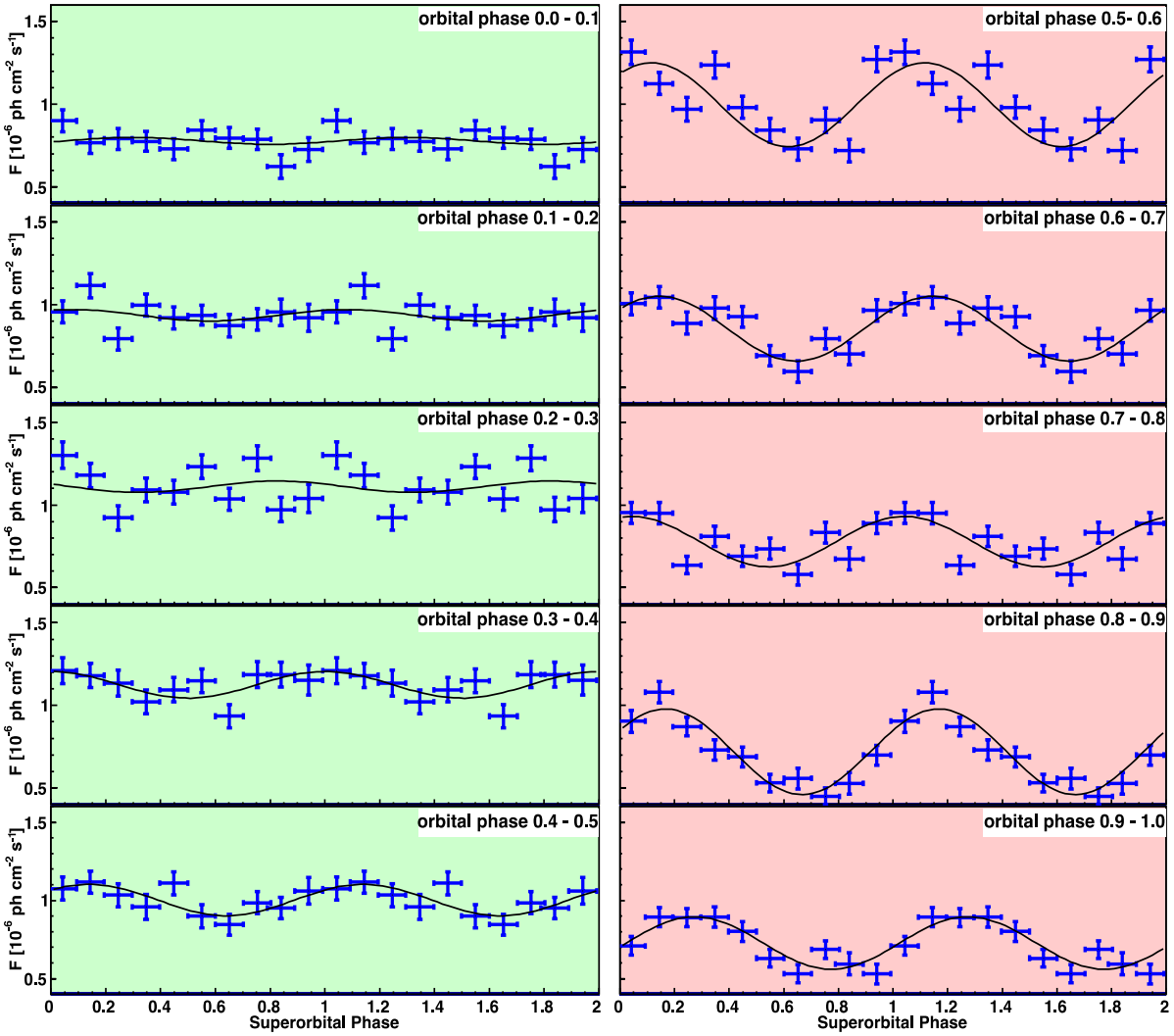

Each panel shows the GeV flux at a fixed orbital position, along a period of 4.5 years

The background represent the region of **periastron** and **apastron**, respectively

Black line: Fit sinusoidal with fixed superorbital period

Zooming in

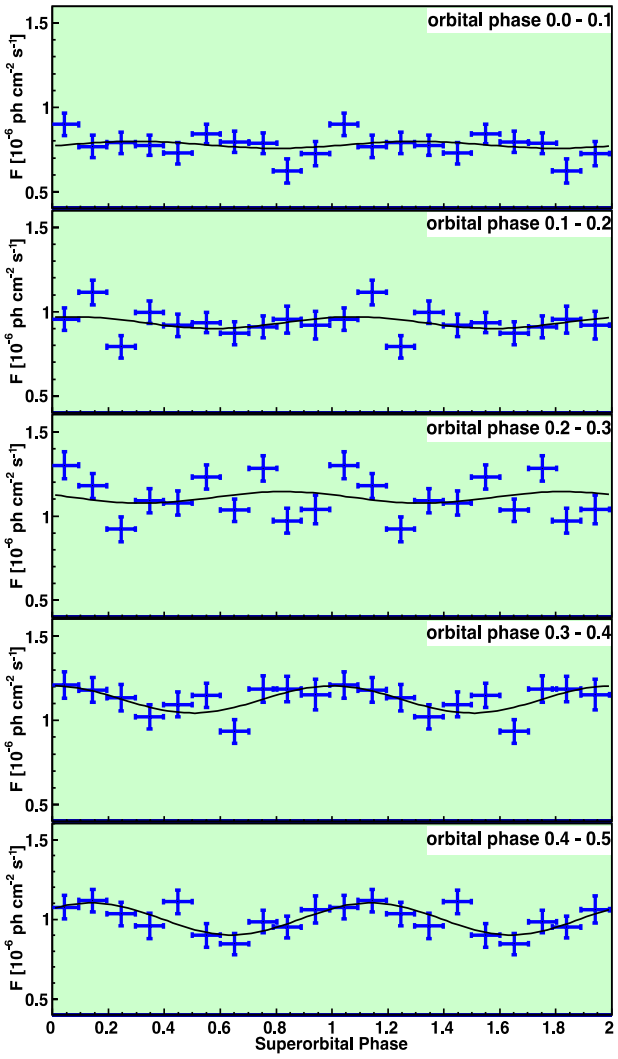

- From orbital phase 0.1 to 0.5, including the periastron region, there is no significant flux variation along the superorbit.
- As soon as we depart from periastron we start to see superorbital variability (see phase 0.5)
- Conditions for GeV generation must not significantly change

Zooming in

- From orbital phase 0.6 to 1.0, including the apastron region, there is significant flux variation in the superorbit.
- The variation is maximal before and after apastron
- Concurrently, **a sine with a fixed period of 1667 days** is at all orbital bins a better fit to the data than a constant
- Close to apastron, the superorbit induces clear variations. GeV emission conditions change.

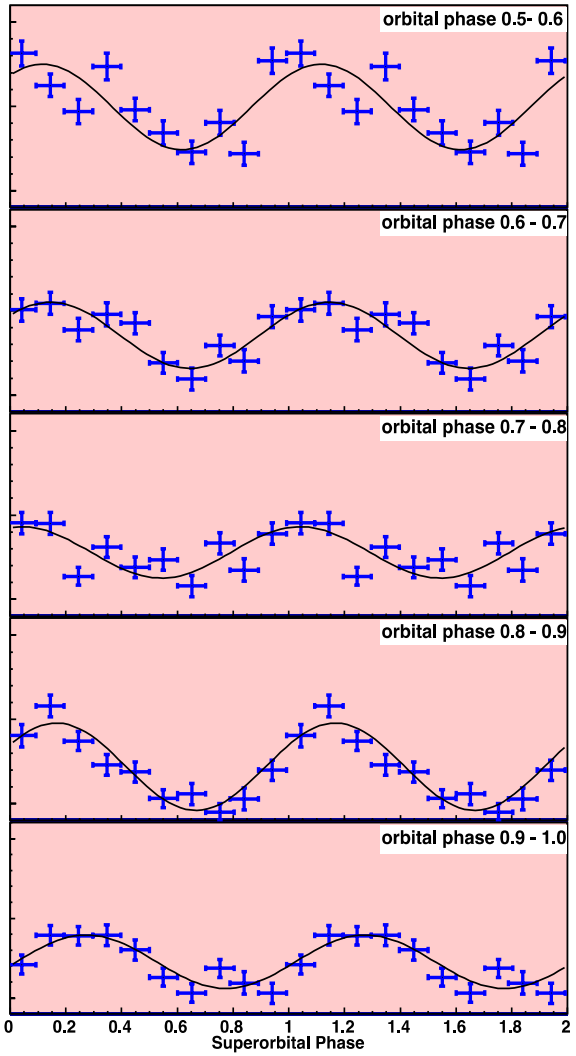

Is the superorbital GeV evolution stable?

- Previous data set: Aug 2008 – March 2013
- New data set with additional data: Aug 2008 – Sep 2015
  - 2.5 years of additional data
  - Reanalysis using newest P8 data and 3FGL catalog
- Data from 100 MeV – 300 GeV
- IRFS: P8R2_SOURCE_V6
- Catalog: 3FGL
- Diffuse model: gll_iem_v06.fits

Additional 2.5 years of data confirms all previous trends

Stable evolution

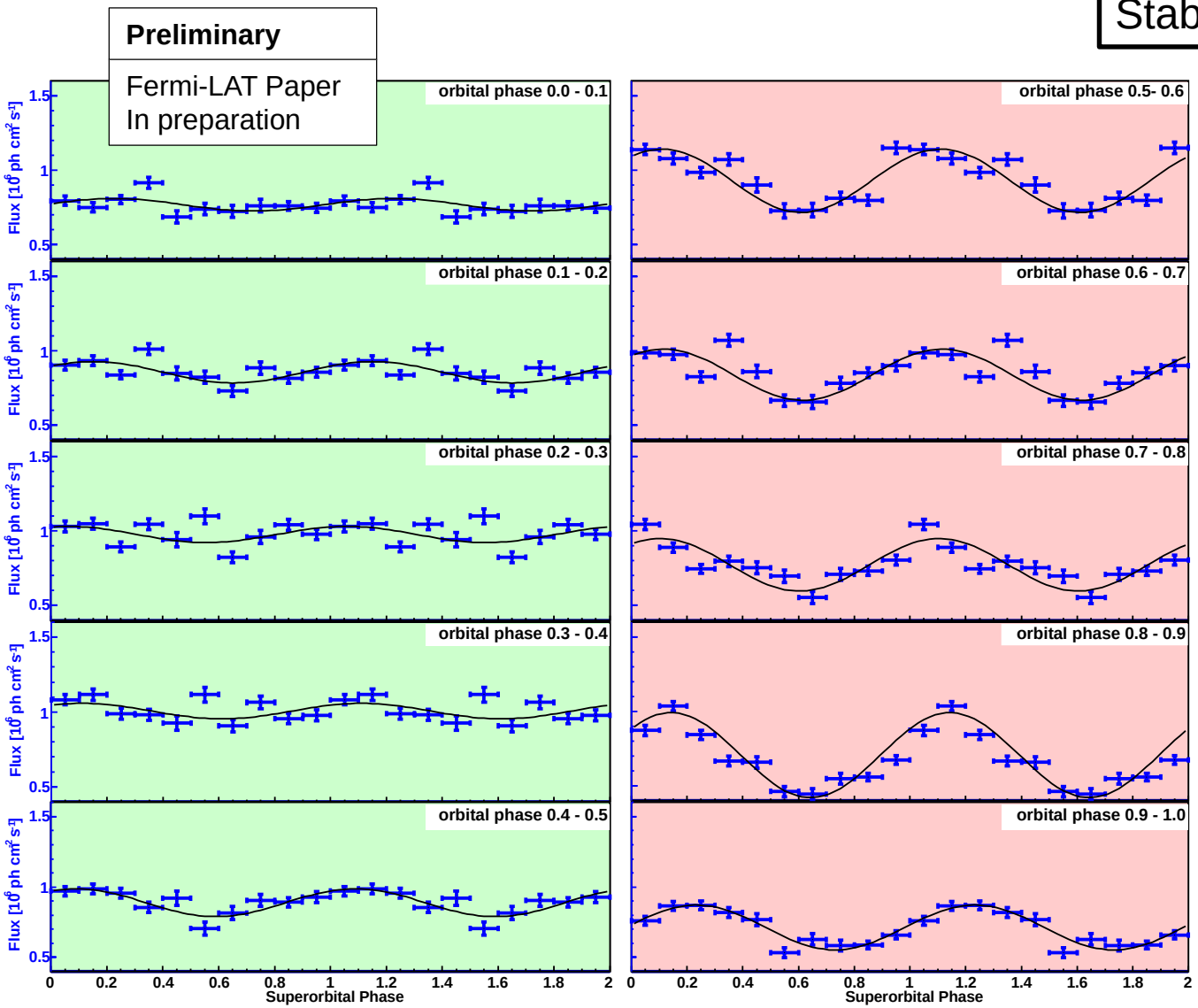

What could be happening?

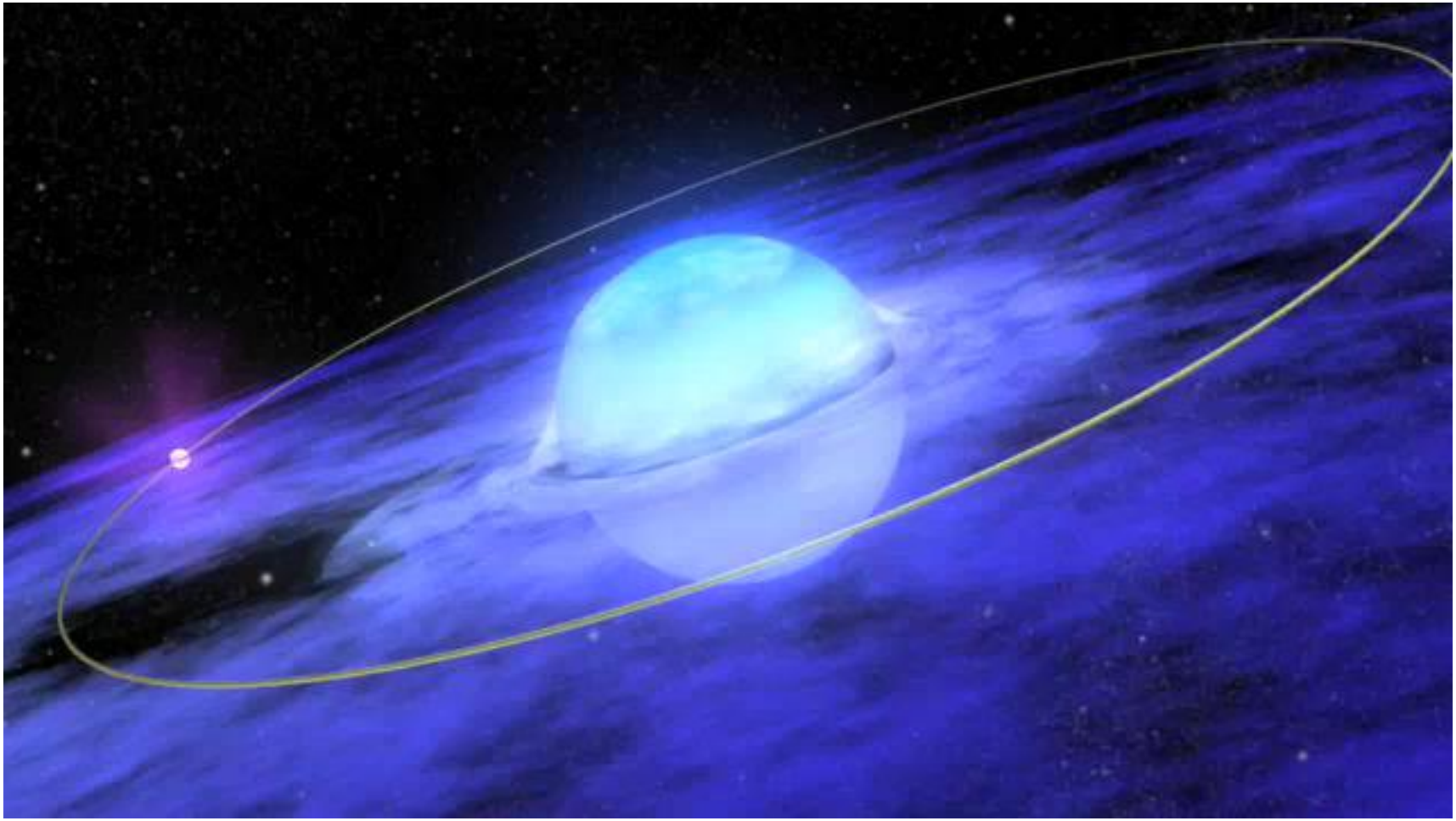

Credit, press release from NASA

Imagine in this movie a quasi-cyclic variability of the extent of the disc
(i.e. of the influence of disc matter ripped off by the NS passage)

What could be happening?

The superorbital variability in Be binary could be understood as a quasi-cyclical increase of the circumstellar disc size or mass decretion rate

The influence of the matter stripped off from the disk by the compact object's passage can be larger and located farther out in periods of higher mass loss

Periods of a relatively smaller disc

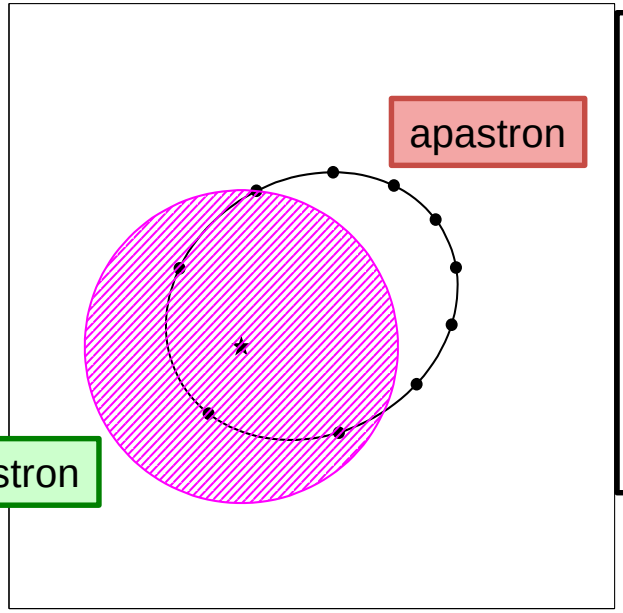

In periastron the influence of the cyclical increase of the disc is minor, since the compact object is always affected by it.

In apastron the influence of the cyclical increase of the disc is larger, but likely not maximal since the disc may not reach to overtake it.

Periods of a relatively larger disc

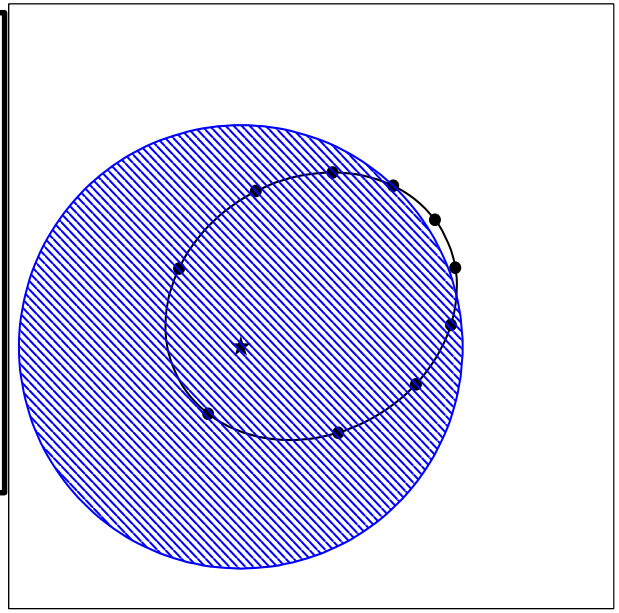

Mass accreted/in the vicinity of the NS changes a lot along the orbit

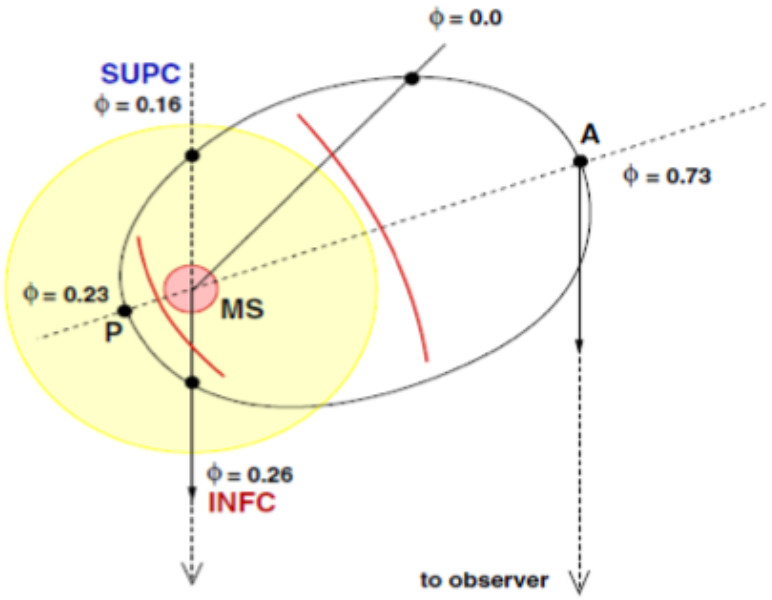

The rate of mass captured by the NS varies with the distance

$dM/dt \sim d^{-2}$ Poloidal wind

$dM/dt \sim d^{-n} \exp[-(d/d_{cut})^{10}]$

e.g., for Be stars, with winds of 2 components, poloidal and equatorial, changes can reach up to 3-4 orders of magnitude

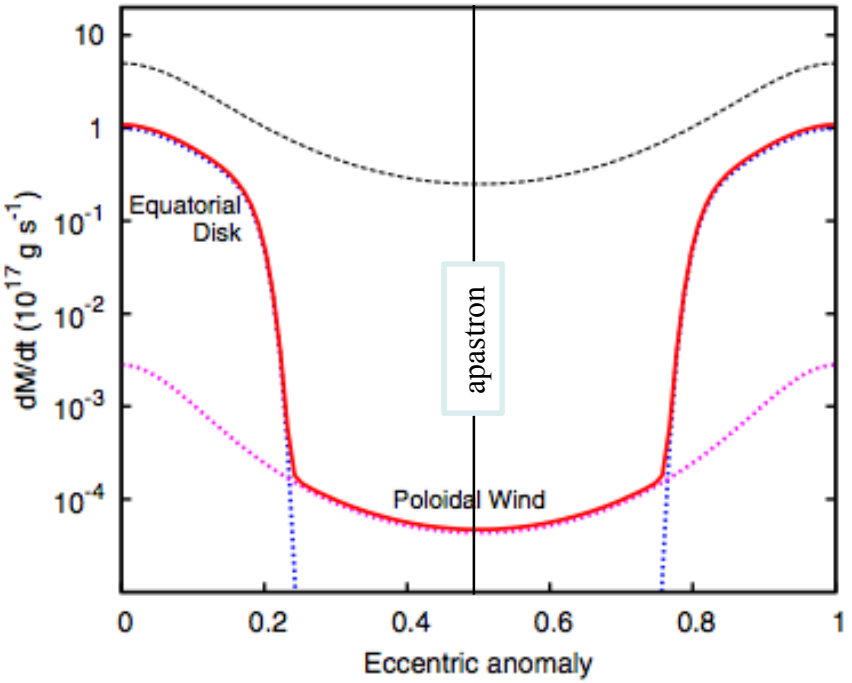

Figure 1. Rate of mass captured by a NS from the equatorial disk (blue dotted line) and the poloidal wind (magenta dotted line) emitted by the Be star in LS I +61°303, as a function of the eccentric anomaly, and for the fiducial values of the relevant parameters (see Table 2). Red solid line is the sum of these two contributions. The black dashed line shows the case of an increased Be star mass-loss rate, $\dot{m}_1^{\max} = 5$, and a disk cutoff beyond the maximum orbital separation, $d_{cut} > a(1+e)$.

See Papitto, DFT, Rea 2012, ApJ

Flip-flop between states is possible depending on the pulsar period

Papitto, DFT, Rea 2012

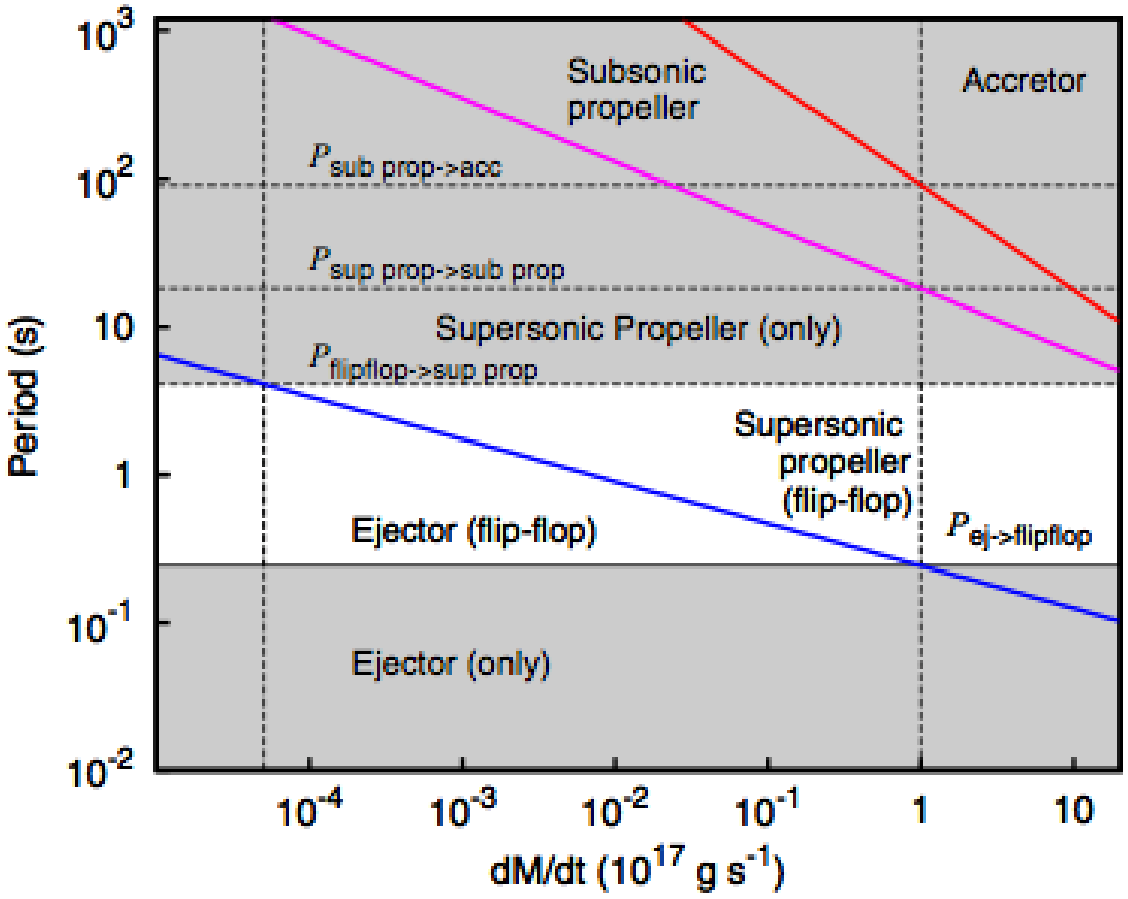

Example for a fixed magnetic field of $B=10^{13}$ G

Flip-flop between states is possible depending on the pulsar period

Papitto, DFT, Rea 2012

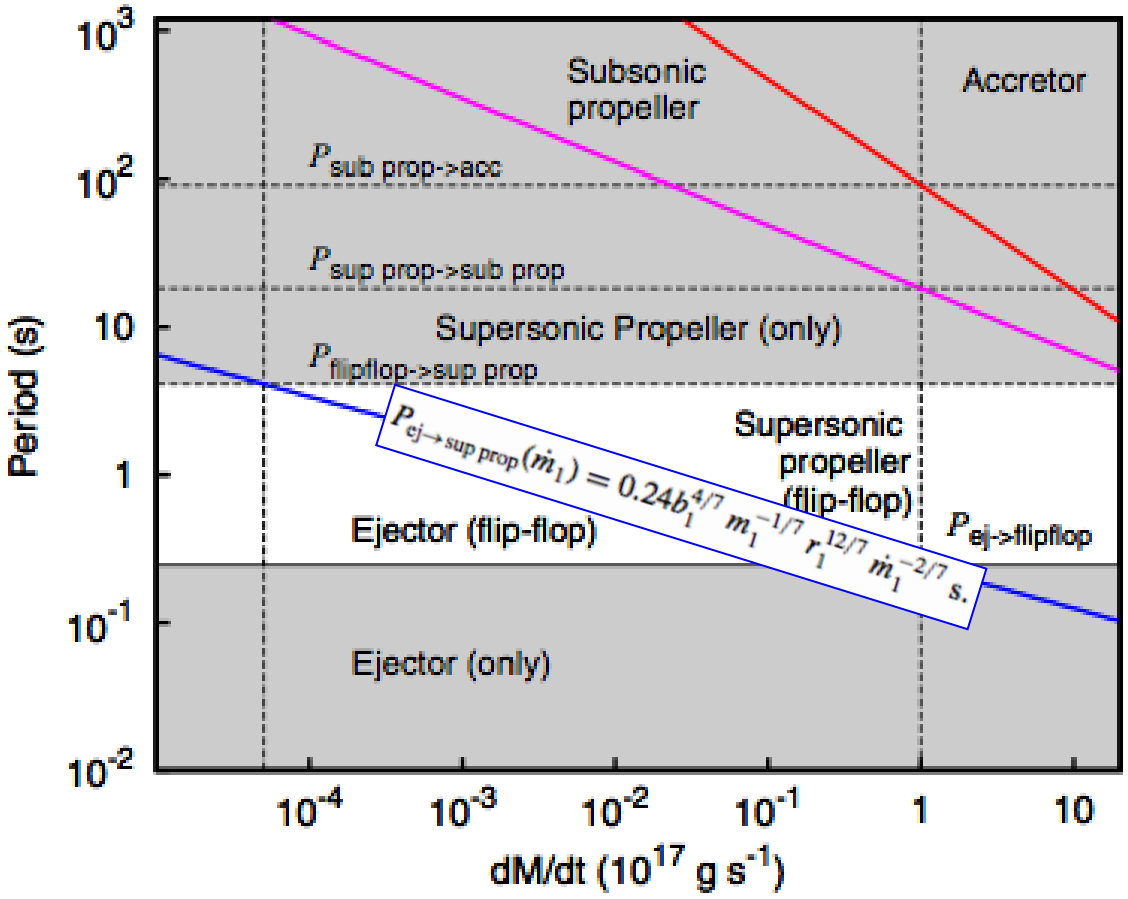

Example for a fixed magnetic field of B=10^{13} G

Parameter space limited by bolometric luminosity

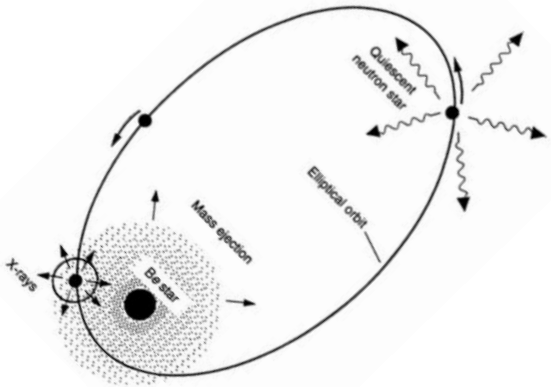

If the apastron luminosity is all ejector-generated the system must be to the left of the red curves

It could always be an ejector or stay flip-flopping along the orbit depending on *(P,B)*

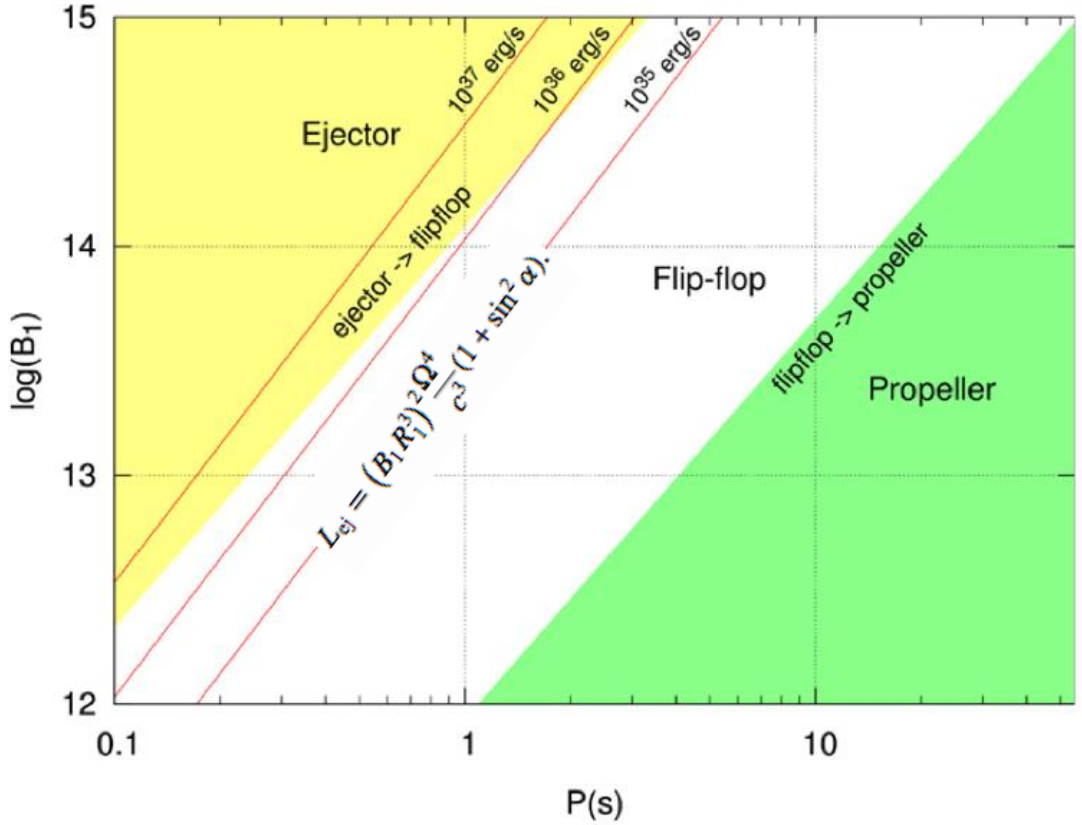

Figure 6. Ejector, *flip-flop*, and propeller states plotted in the NS magnetic field vs. spin period phase space, evaluated for a NS in LS I +61°303 and for the fiducial values adopted for the maximum and minimum mass capture rate ($\dot{m}^{\max} = 1, \dot{m}^{\min} = 1$). From top to bottom, the red solid lines mark the relation between the period and the magnetic field of the NS when the ejector luminosity is 10^{37}, 10^{36}, and 10^{35} erg s^{-1}, respectively, and the magnetic offset angle is $\alpha = 45°$.

Parameter space limited by bolometric luminosity

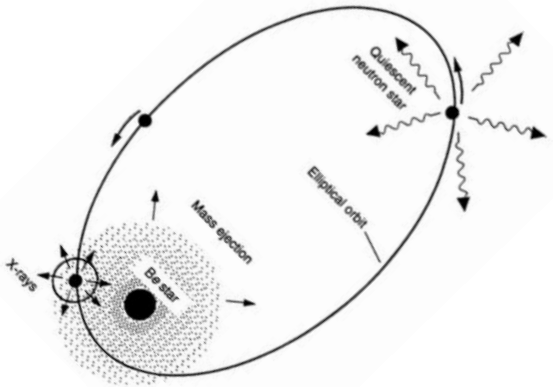

Yellow limit:
At periastron (max accretion rate) the system starts to be a propeller

Green limit:
At apastron (min accretion rate) the system starts to be propeller (and then it'll always be along the orbit)

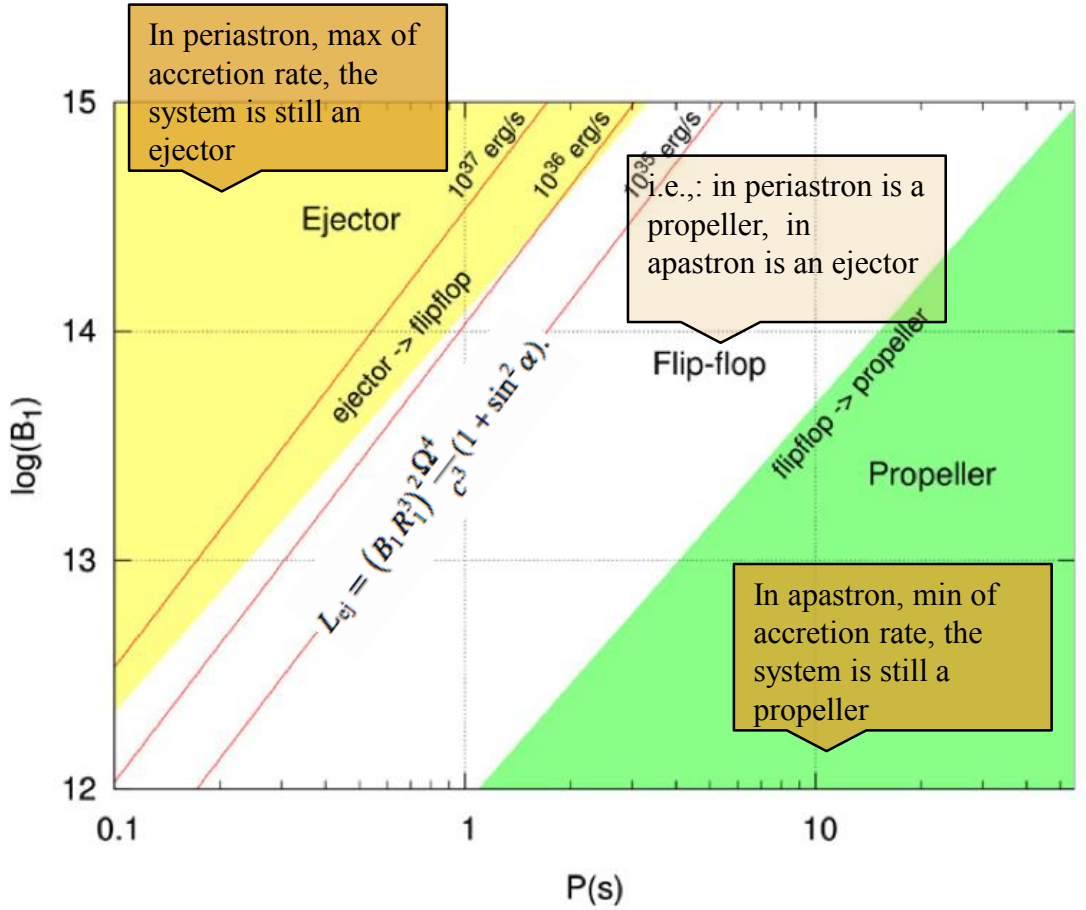

Figure 6. Ejector, *flip-flop*, and propeller states plotted in the NS magnetic field vs. spin period phase space, evaluated for a NS in LS I +61°303 and for the fiducial values adopted for the maximum and minimum mass capture rate ($\dot{m}^{\max} = 1, \dot{m}^{\min} = 1$). From top to bottom, the red solid lines mark the relation between the period and the magnetic field of the NS when the ejector luminosity is 10^{37}, 10^{36}, and 10^{35} erg s^{-1}, respectively, and the magnetic offset angle is $\alpha = 45°$.

Parameter space limited by imposing superorbital variability

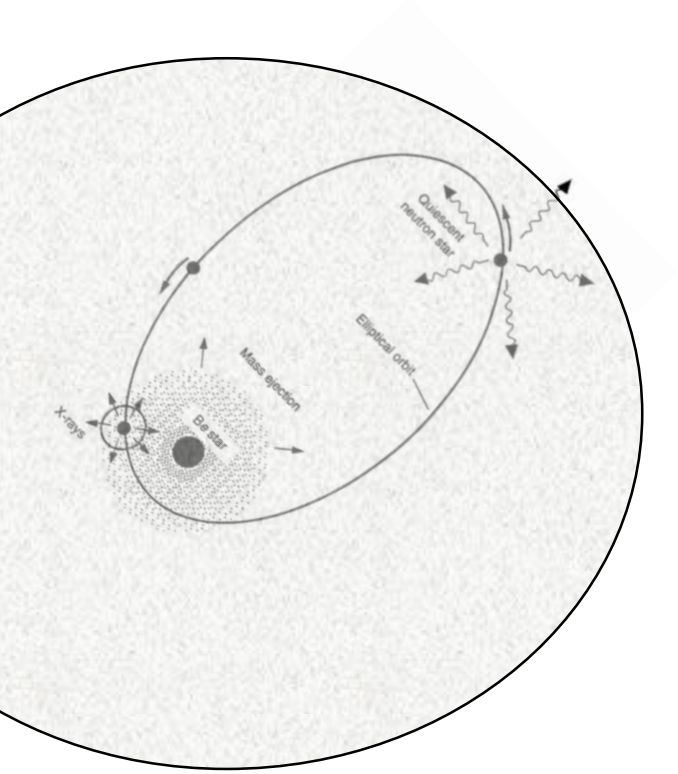

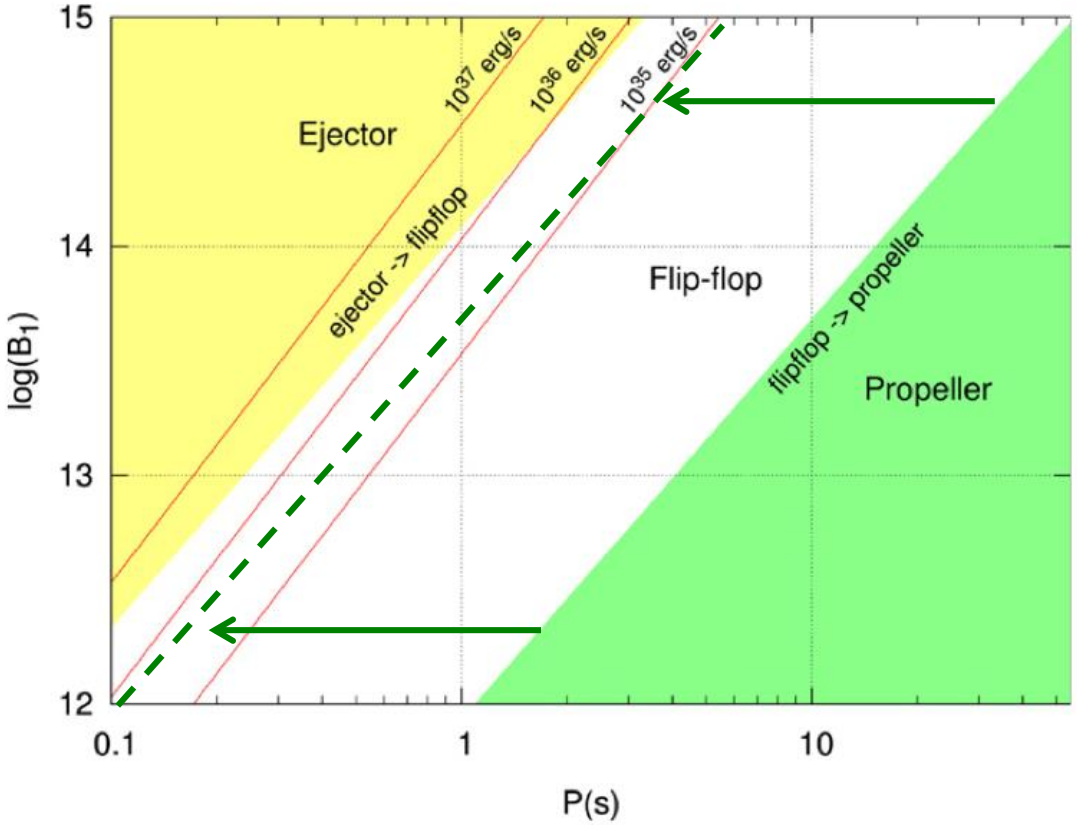

If the disc dominates the apastron (suppose: having grown larger at the maximum of the superorbital variability); the transition to the propeller moves to the left, and depending on *(P,B)* the system could be a permanent propeller (to the right of the green line) or a flip-flopper (to the left)

If this happens, what was to expect?

- If it is a flip-flopping system, it would be natural to expect significantly reduced TeV radiation near apastron for super-orbital phases of ~ 1 ± 0.2.
    - The TeV emission would be quasi-cyclic.

- If we can track the accretion rate onto the compact object, the TeV emission will be anti-correlated with it.
    - This would be valid both in an orbit-to-orbit basis, as well as in longer timescales.
    - But how to track the accretion rate onto the neutron star reliably?

- If there is ever a large or a giant flare observed from LS I +61 303 which allows for enough counts to be collected, we should detect a pulsating period in a range where flip-flopping is possible.

Torres et al. 2012, Papitto, DFT, Rea 2012, both in ApJ

TeV photons measured along a decade

A 4-years (2010-2014) campaign with the MAGIC telescopes; plus use of archival MAGIC data and published VERITAS data

TeV data covers 2006-2015

Search of (anti-)correlation between the TeV emission and the Be star mass-loss rate: MAGIC data from orbital Phase = 0.8 – 1.0 LIVERPOOL optical data (some strictly simultaneous observations)

Spectral studies: Entire sample, data split according superorbital and orbital phase and flux levels: *shows no significant variation of spectral properties at any scale*

Result: modulation in timescales of 4.5 years happens also at TeV

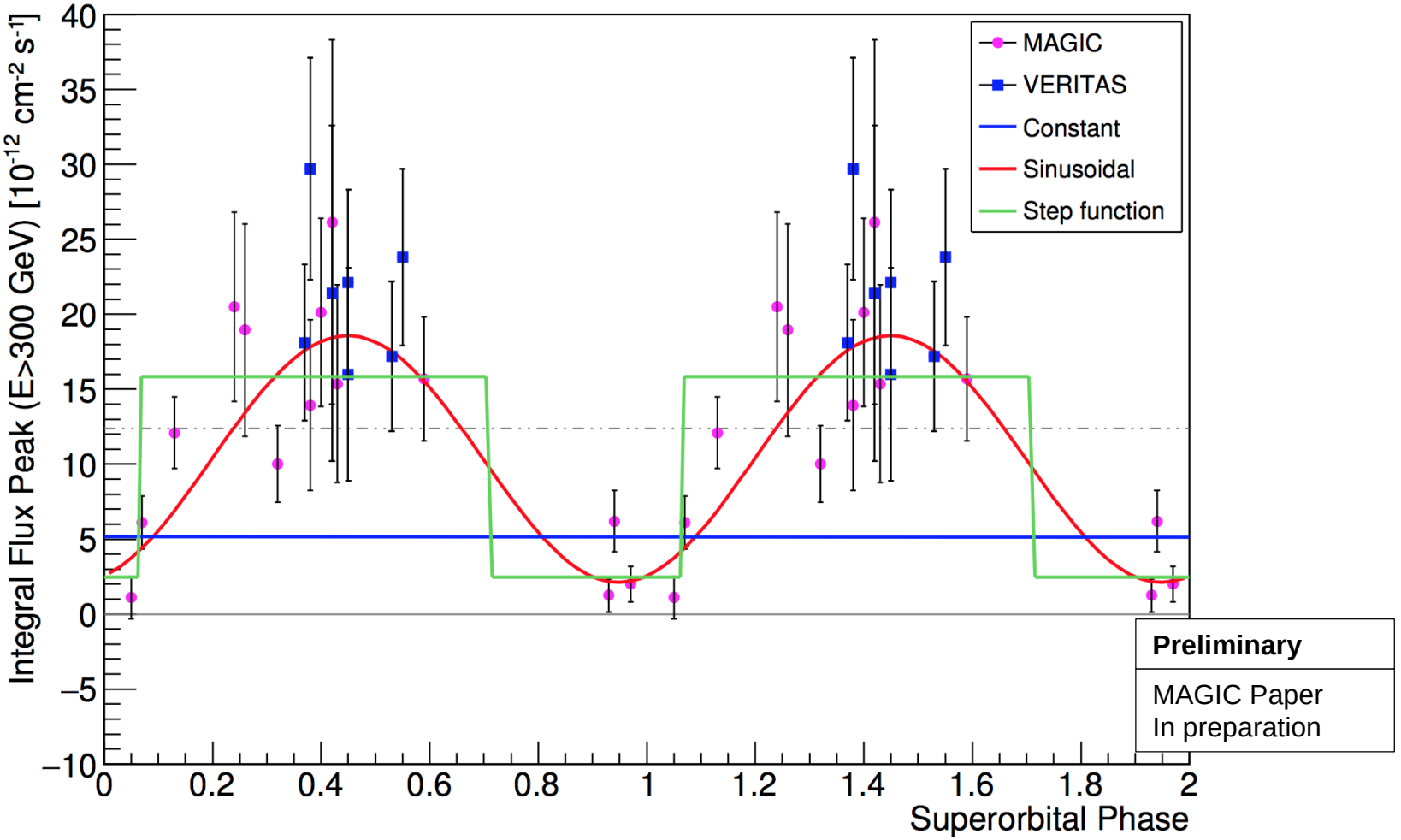

Monitoring for almost a decade: amplitude of VHE periodic peak show two states, in a **modulation compatible with the superorbital phase**

In agreement with the prediction.

Too much scattering in the intra-night Hα for a correlation analysis

Correlations between the TeV flux obtained by MAGIC and the Hα parameters (EW, FWHM and vel) measured by LIVERPOOL in the orbital interval 0.75 – 1.0.

Each data point represents a 10 minute observation in the optical and a nightly flux in TeV.

Blue: nightly, red: 3-hour difference, green: strict simultaneity.

The relation between the mass-loss rate of the star and TeV emission cannot be confirmed with the current generation of telescopes: integrations the observations (order of minutes in optical and order of hours in TeV) and scattering of optical data are a problem.

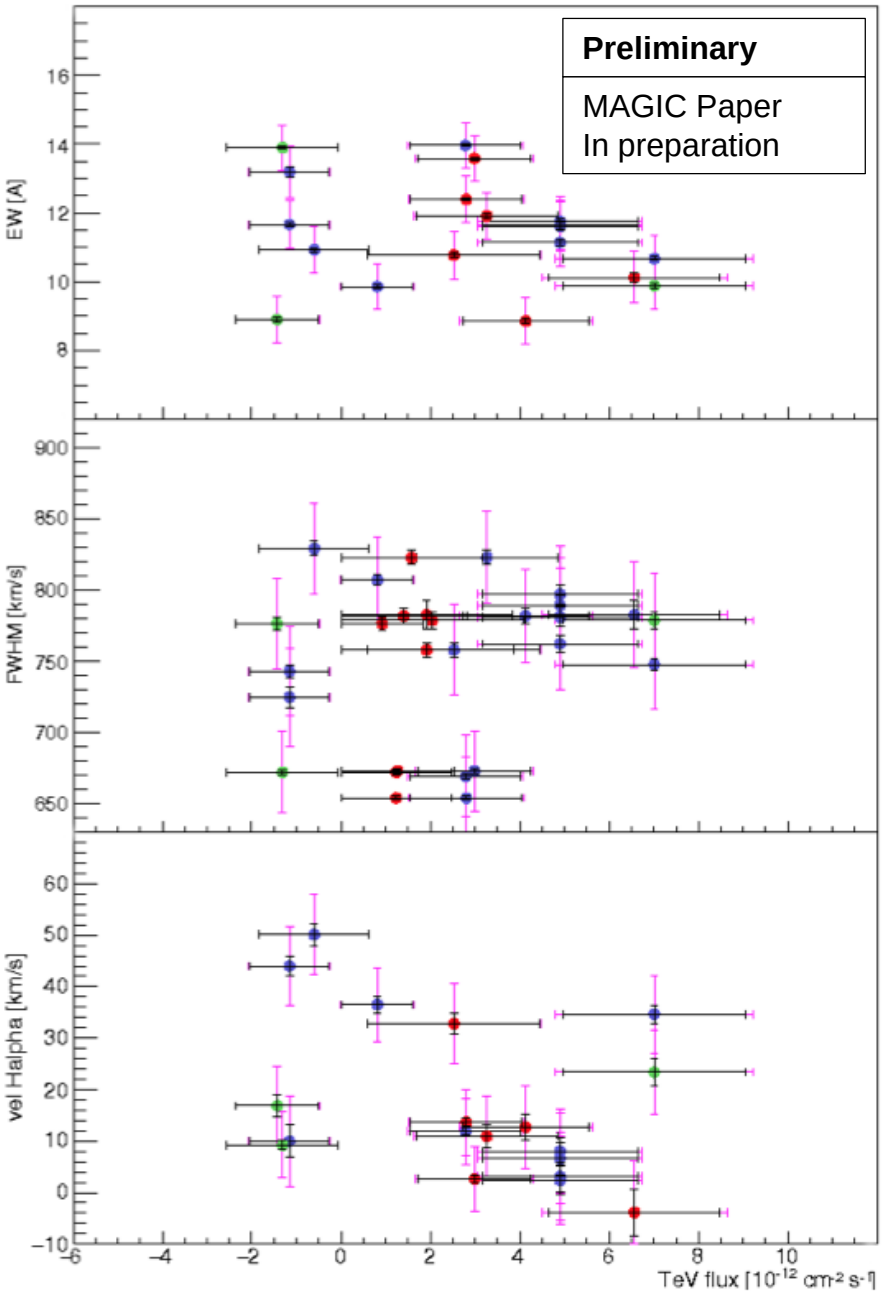

Ha data along several years (1994-2015)

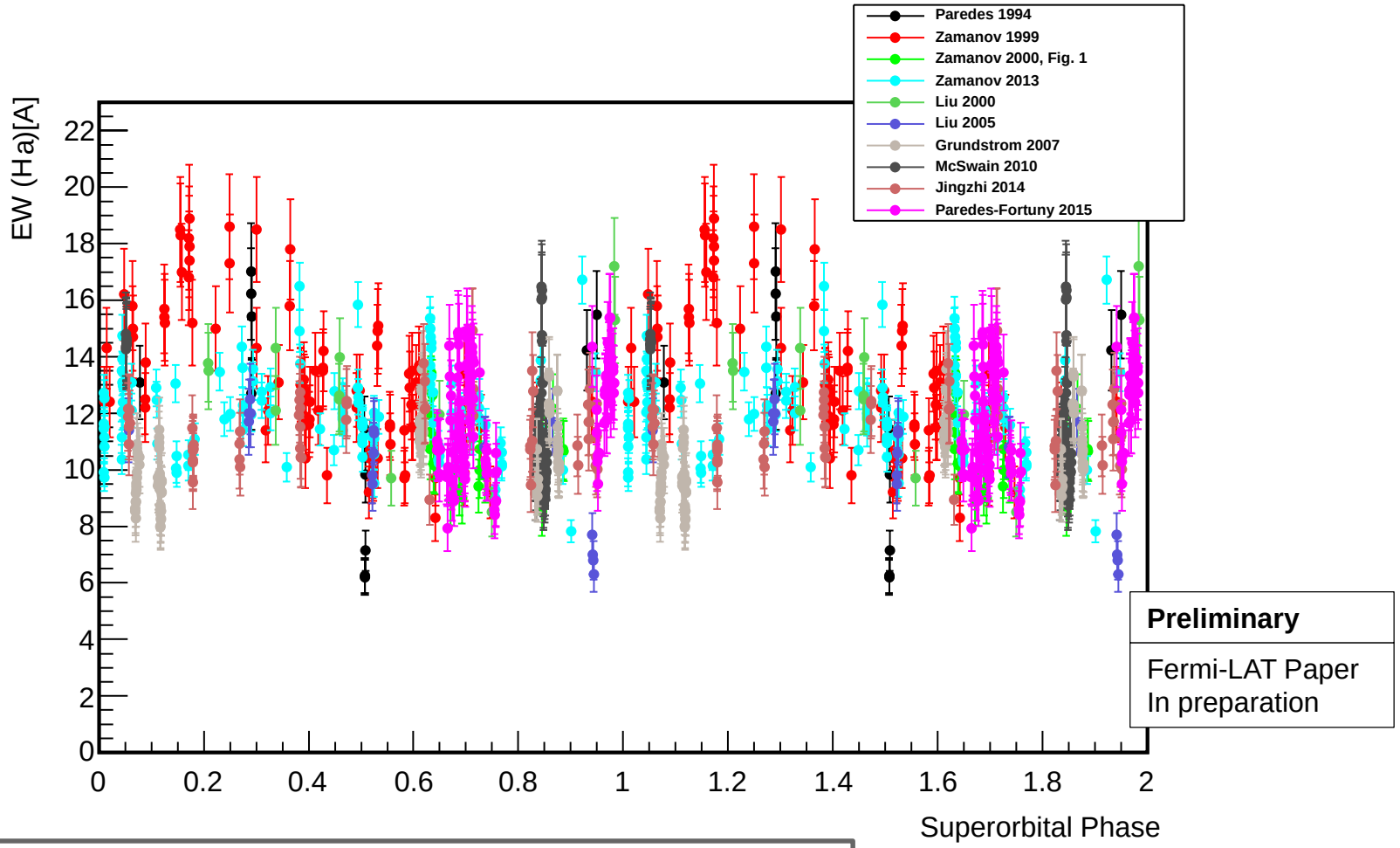

- Equivalent width of Ha emission line showed superorbital variability after one superorbit
- Strong intra night variability

Ha data along several years folded into the superorbit

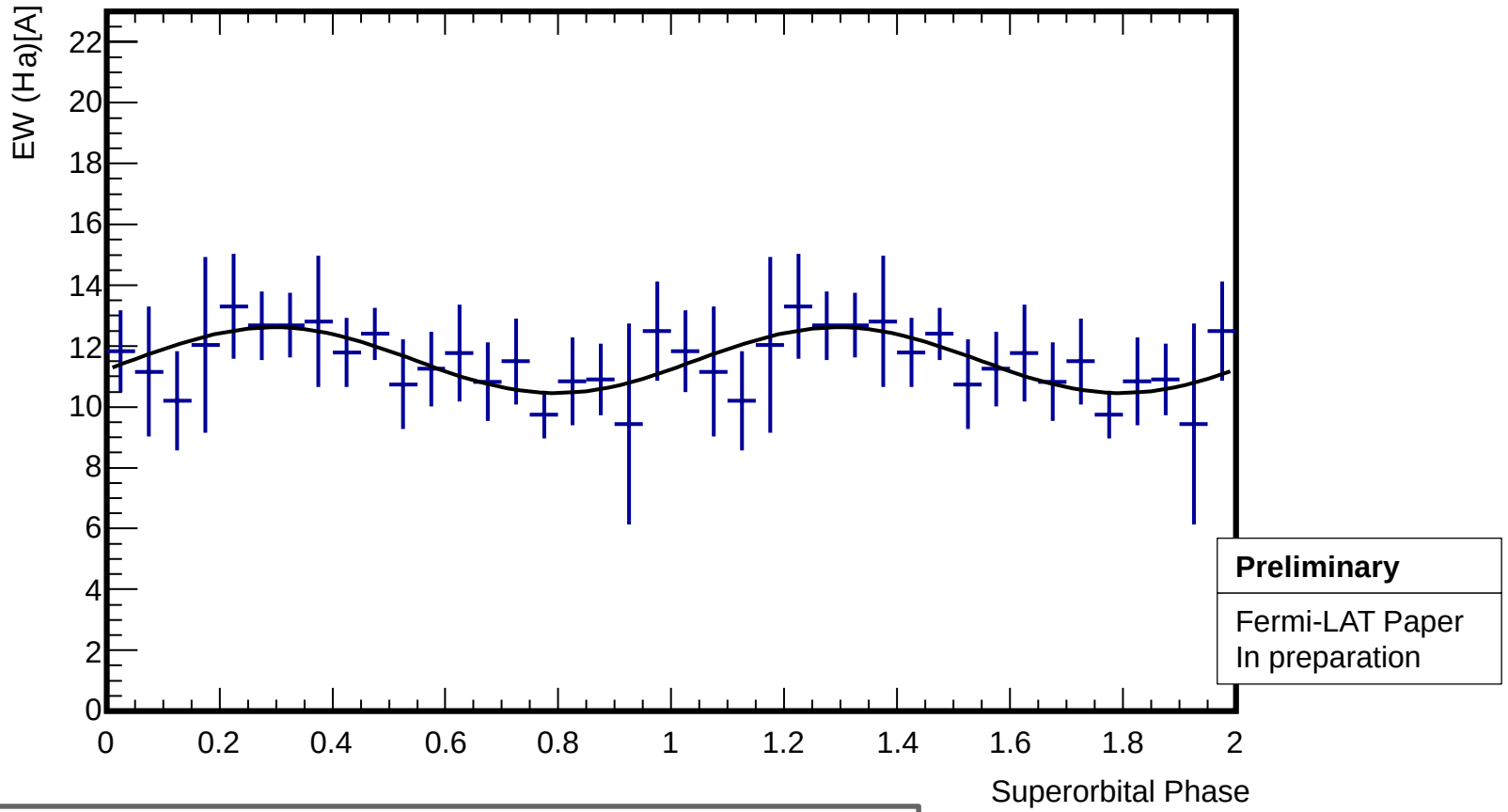

- Data binned into 0.05 of superorbit (error = RMS)

→Probability that EW (Ha) evolution is a random result: 0.02

→ **EW (Ha) is variable along the superorbit**

EW Hα in the superorbit compared with GeV

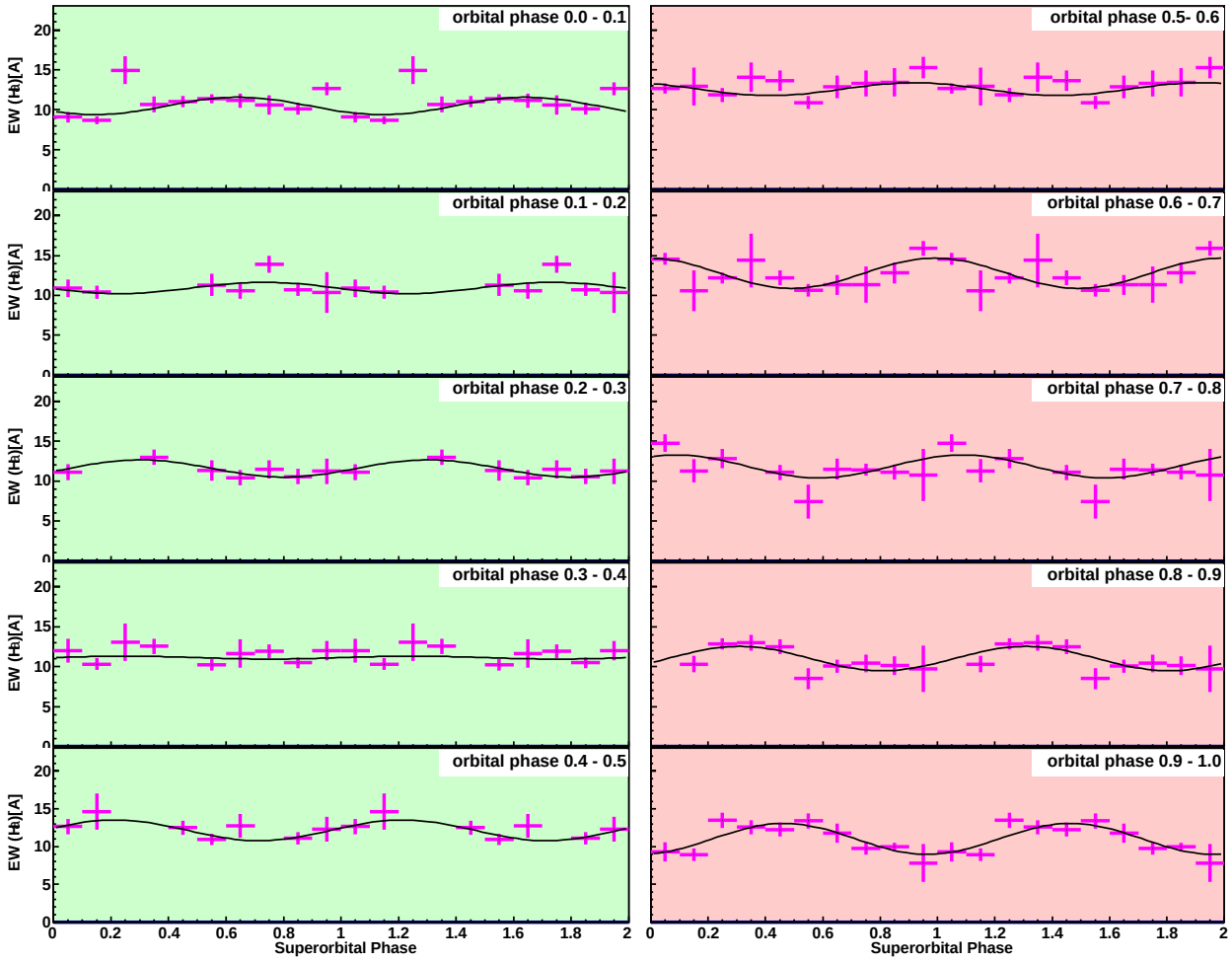

Preliminary

Fermi-LAT Paper
In preparation

Same folding like in GeV

→Modulation also here visible around apastron

Concluding remarks

- The system seems to be formed by a pulsar and a Be star, subject to some sort of quasi-cyclical variability at all frequencies
  - flip-flop btw propeller and ejector seems to provide a good overall handle of phenomenology
  - period and magnetic field of the pulsar?
- Superorbital modulation detected in all wavelengths studied
  - GeV behavior is stable along the last 7+ years of constant monitoring
- All wavelengths show a modulation distinguishing the apastron from the periastron regions
  - **Radio:** GeV → Correlation at level of 3 sigma (Pearson corr. Coeff.)
  - **X-rays:** no clear (anti)correlation with GeV visible. Emission shifted wrt GeV?
  - **EW(Ha):** Show superorbital modulation around apastron
  - **TeV:** superorbital behavior discovered, and compatible with flip-flop states
- Possible connection to cyclic mass-loss phenomena in Be stars
  - But yet unclear correlations with tracers
  - The system presents a rich intra-night variability

EW Hα in the superorbit compared with GeV

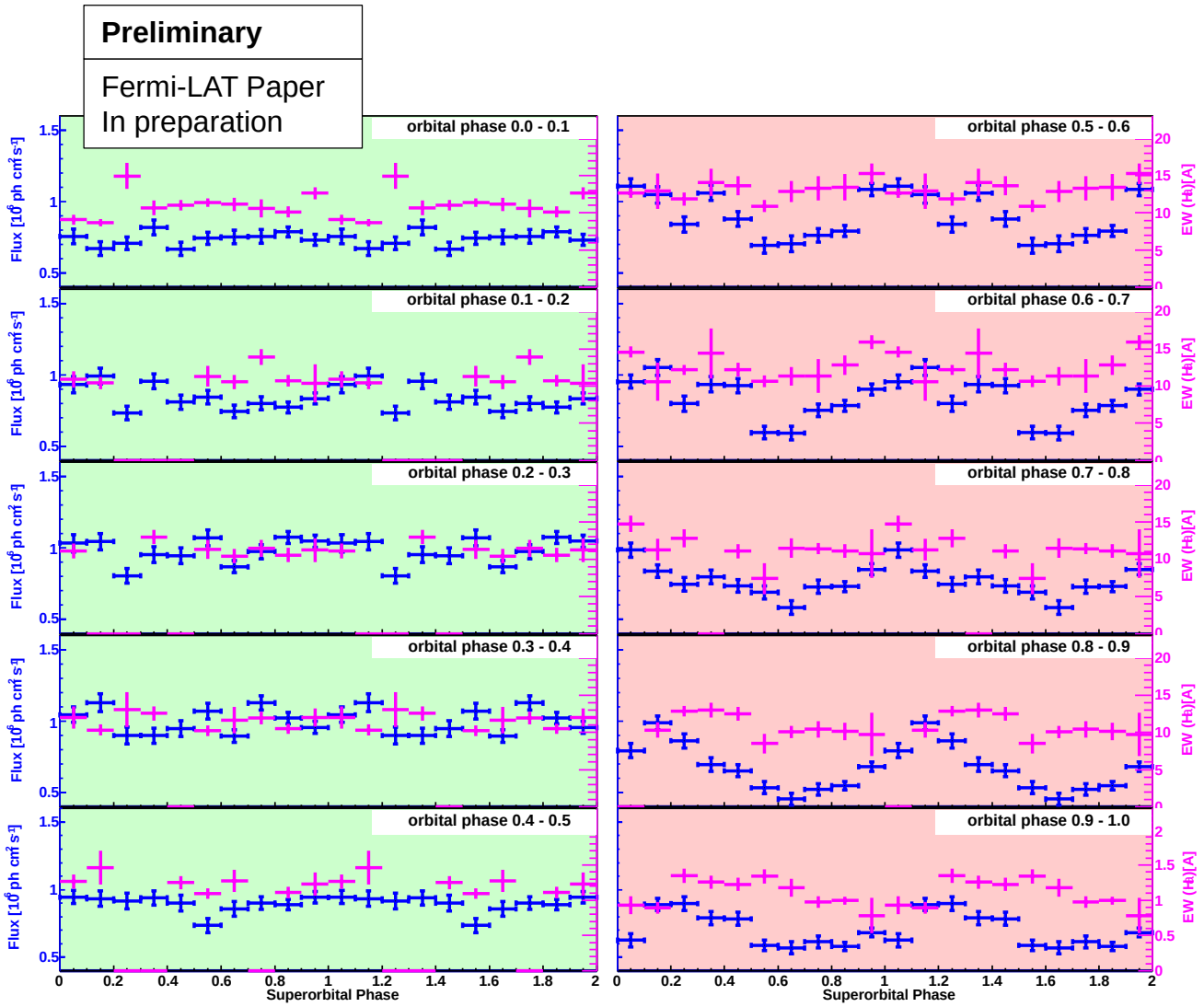

No clear correlation visible between Hα and GeV data

Super-orbital modulation in X-rays

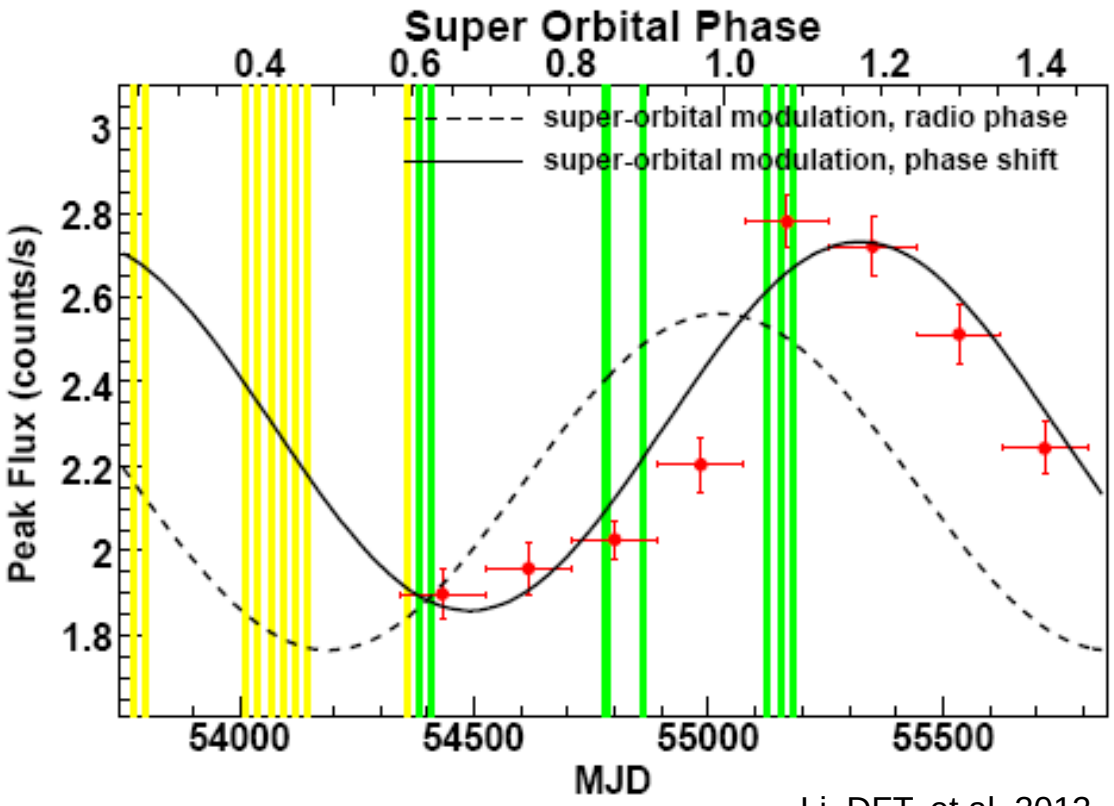

Li, DFT, et al. 2012

Dotted line: behavior in radio
Solid curve: sinusoidal fit to X-ray data (red) obtained with a fixed period to 1667 days
Green (yellow) boxes: TeV emission in low (high) state

X-ray emission present a similar behavior when zoomed in

RXTE data

3-30 keV

2007 - 2011

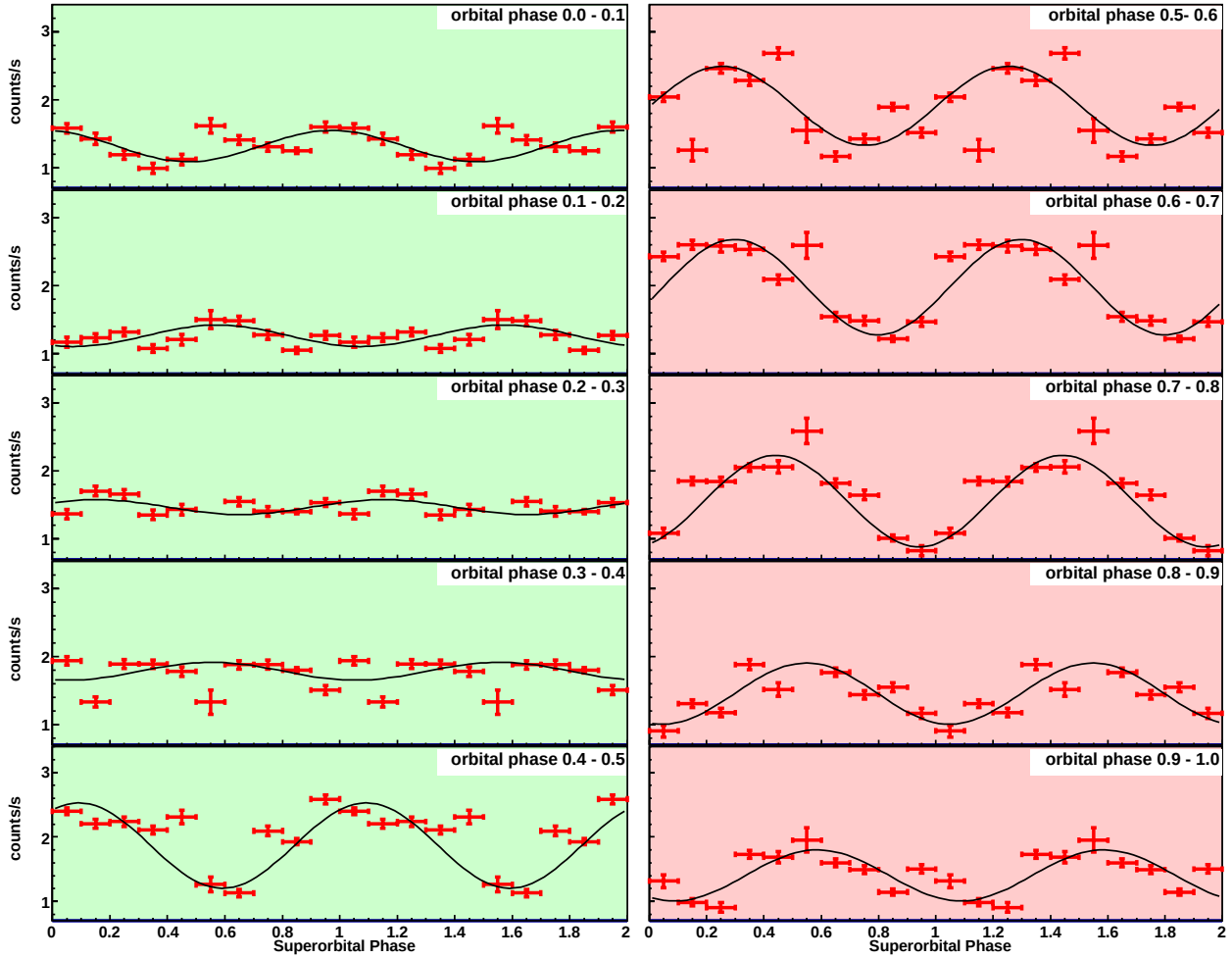

Preliminary

Fermi-LAT Paper
In preparation

Modulation visible around apastron, like in GeV

Black line: Sinusoidal fit with fixed superorbital period

No clear correlation of X-rays with the GeV emission

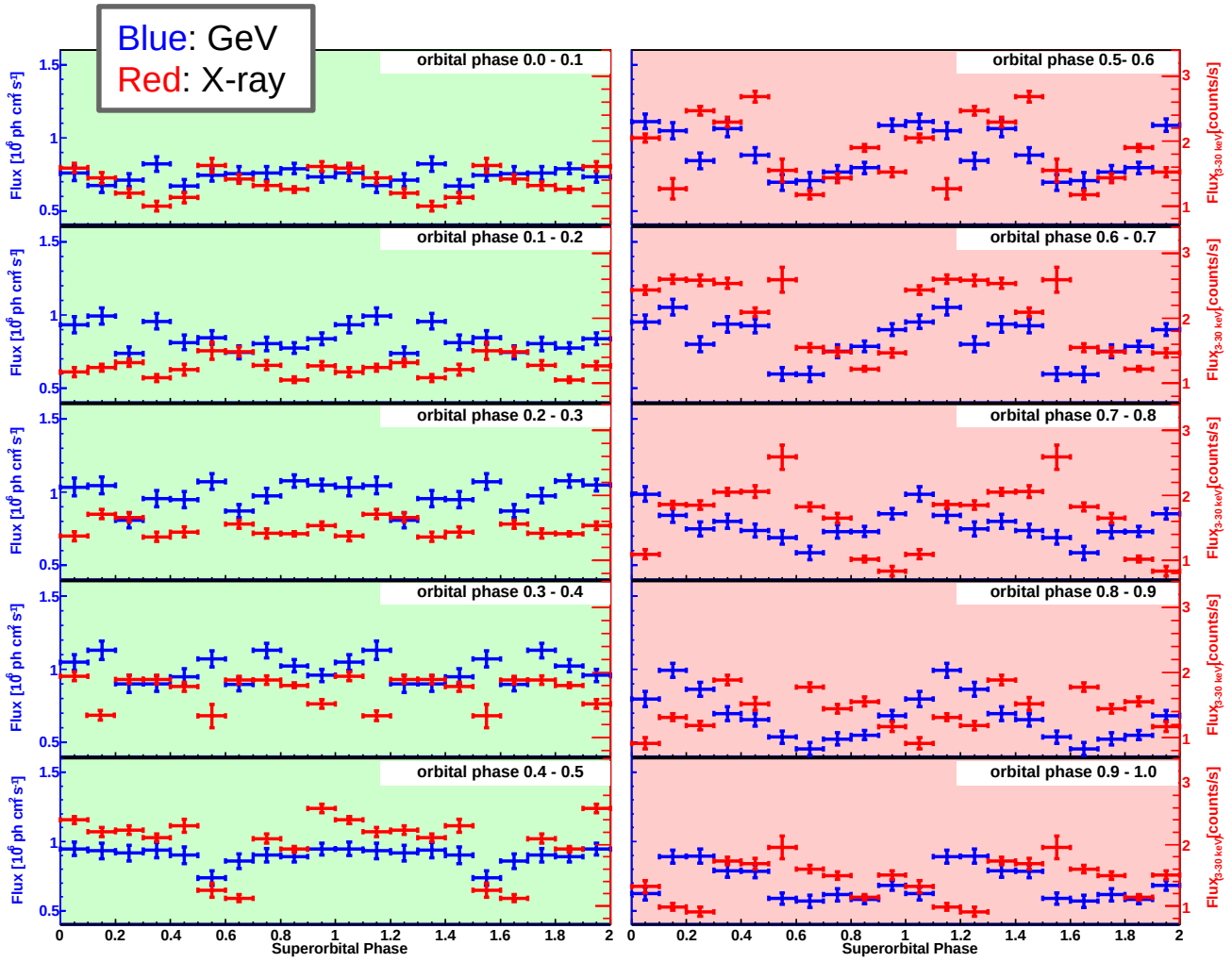

Preliminary

Fermi-LAT Paper
In preparation

Pearson Corr. Analysis reveals **No significant correlation** nor anticorrelation

X-ray emission shifted wrt GeV?

Radio @ 2.25 GHz (GBI data, 1994-2000)

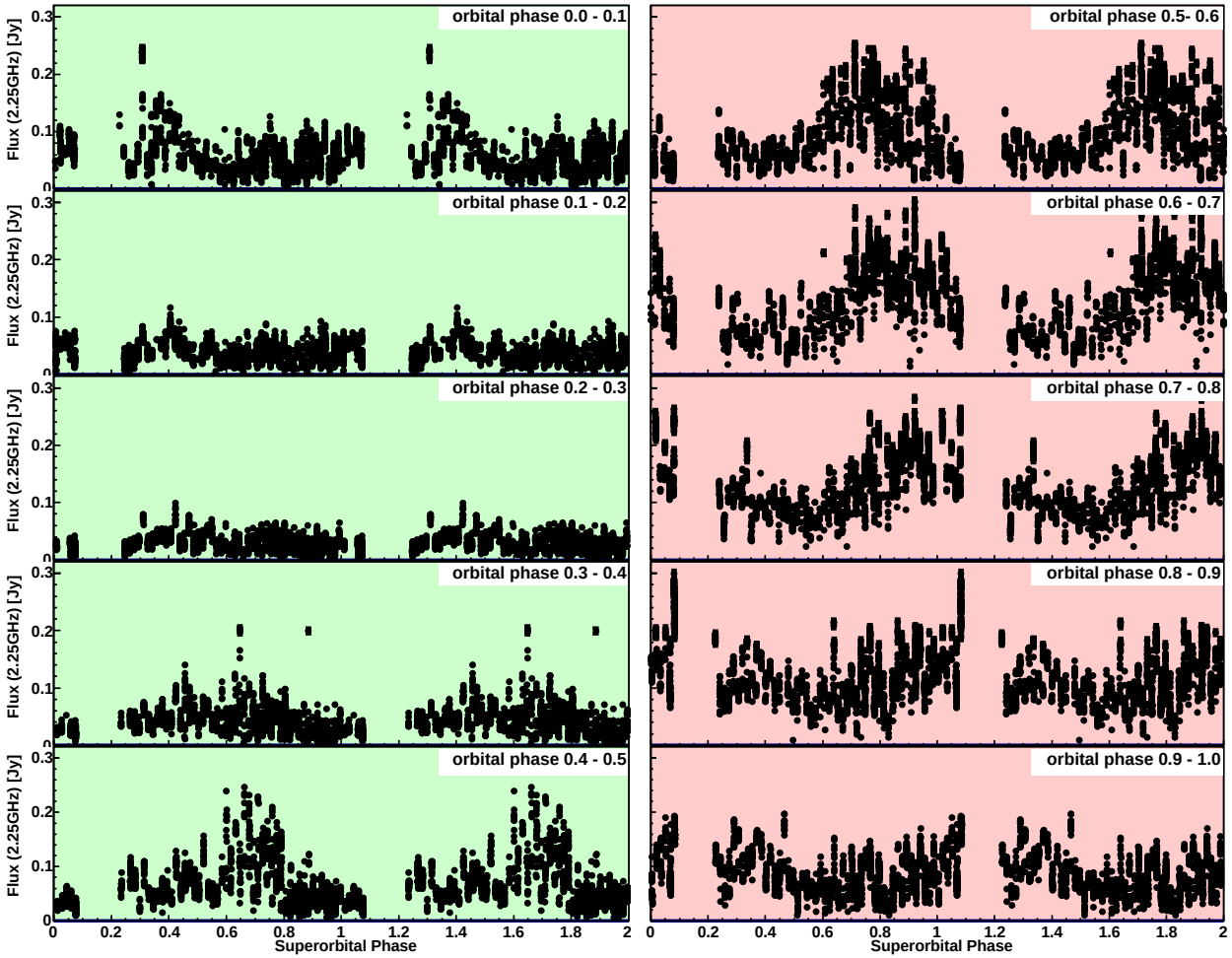

Preliminary

Fermi-LAT Paper
In preparation

Same folding like in GeV

→Modulation visible around apastron

→Modulation starting earlier in orbital phase than in GeV?

Radio @ 8.3 GHz

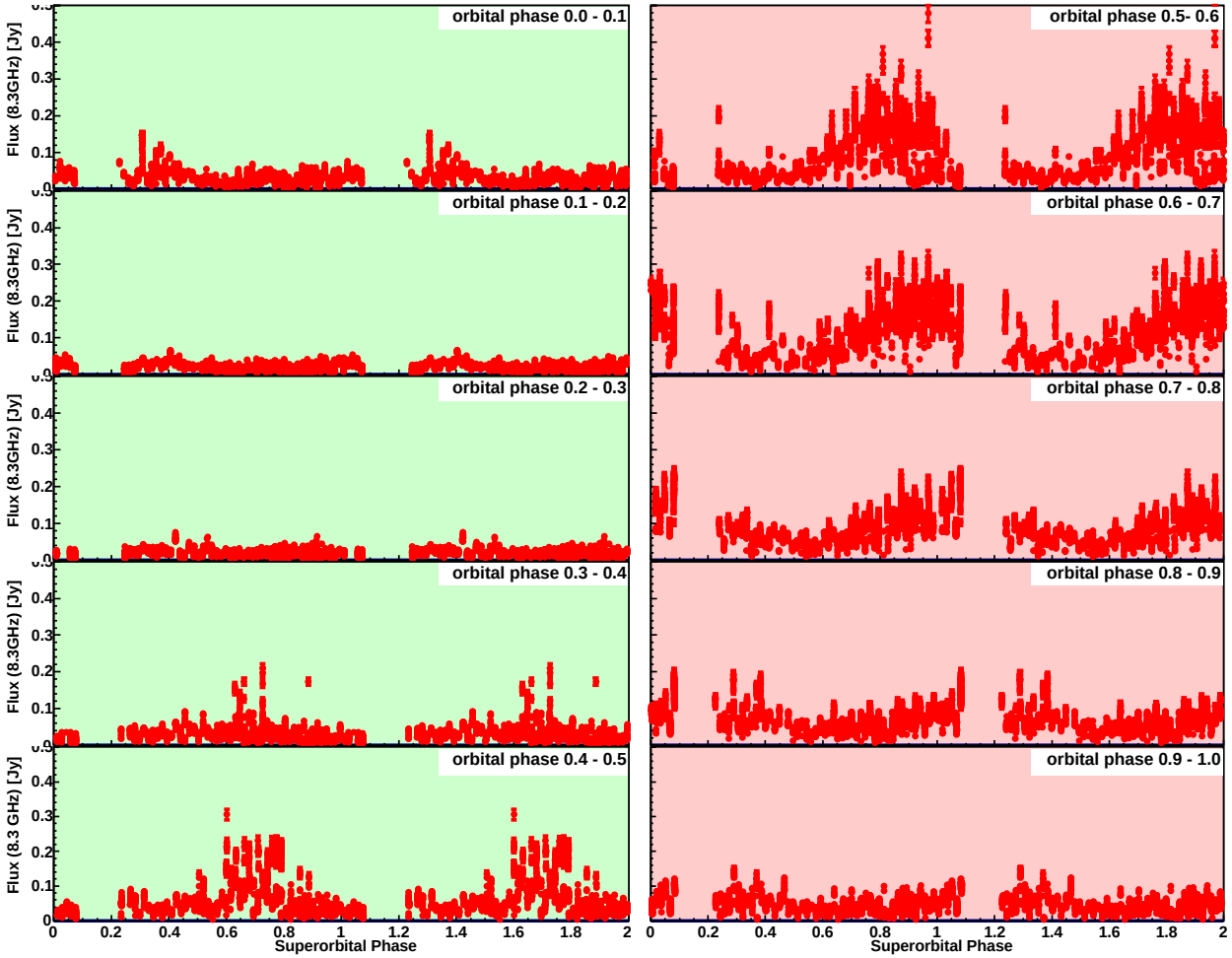

Preliminary

Fermi-LAT Paper
In preparation

Same folding like in GeV

→Modulation visible around apastron

→Modulation starting earlier in orbital phase than in GeV?

Radio in stereo

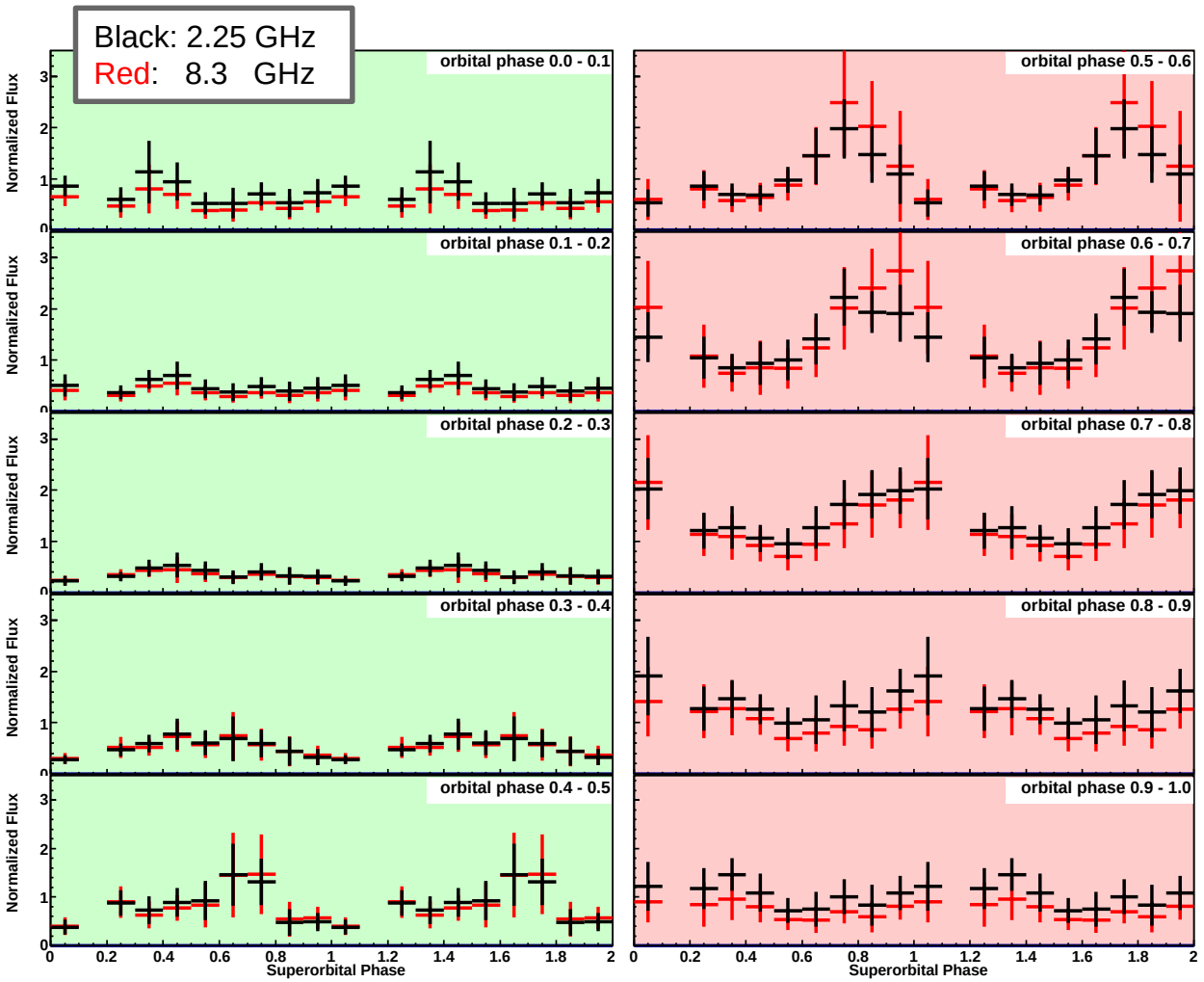

Preliminary

Fermi-LAT Paper
In preparation

Average radio data in superorbital bins of 0.1

Error = RMS

Both frequencies show almost same behavior

Modulation visible around apastron, like in GeV

GeV vs Radio

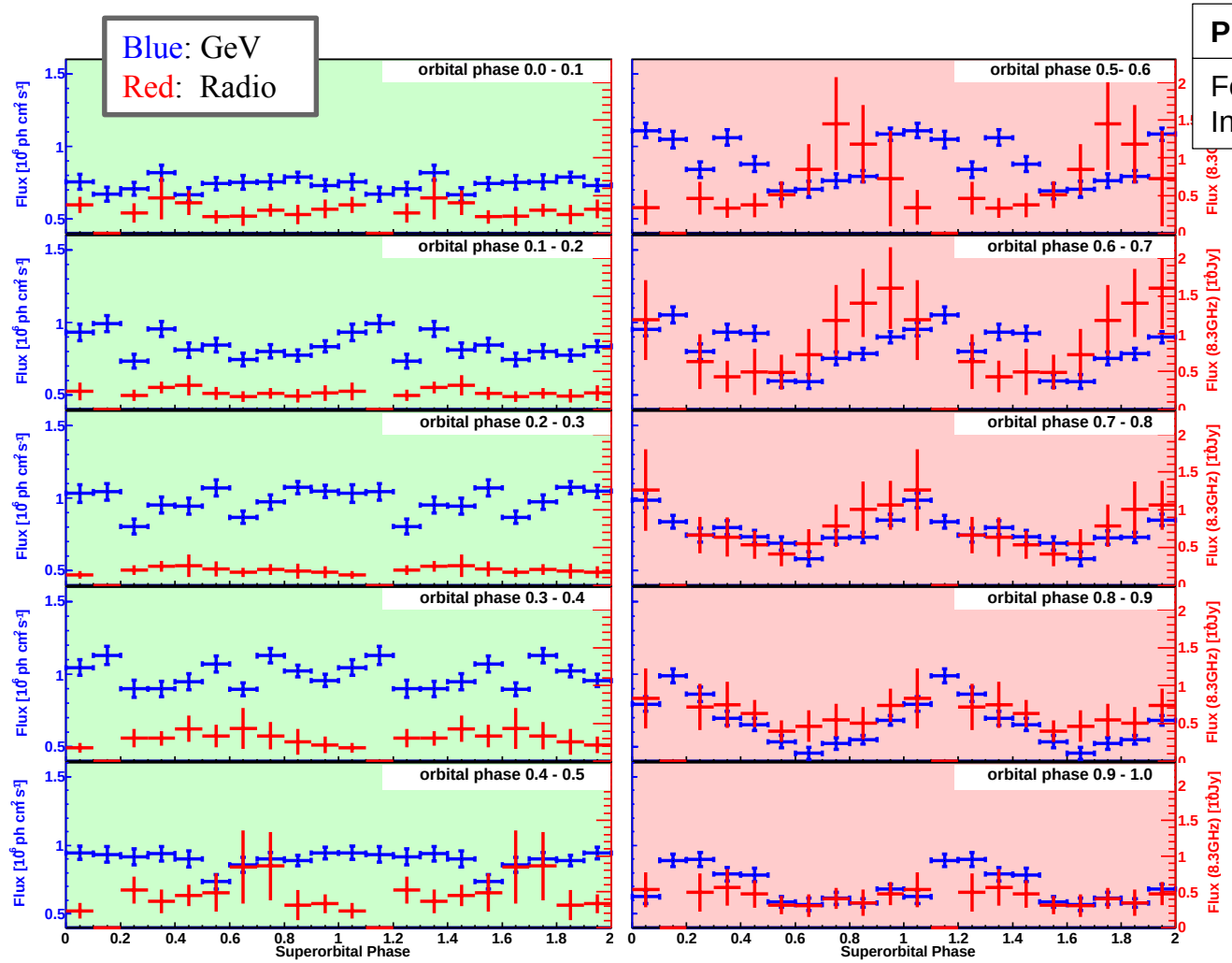

Preliminary

Fermi-LAT Paper
In preparation

Pearson Corr. Analysis reveals a correlation GeV – Radio at the 3σ level around apastron

Additional 2.5 years of data confirms all previous trends

Stable evolution

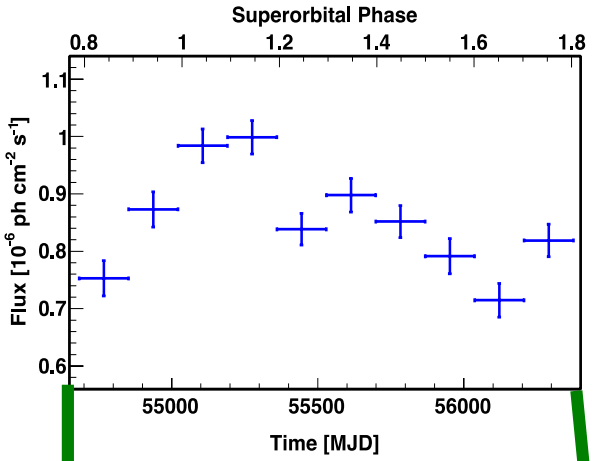

Ackermann et al. 2013

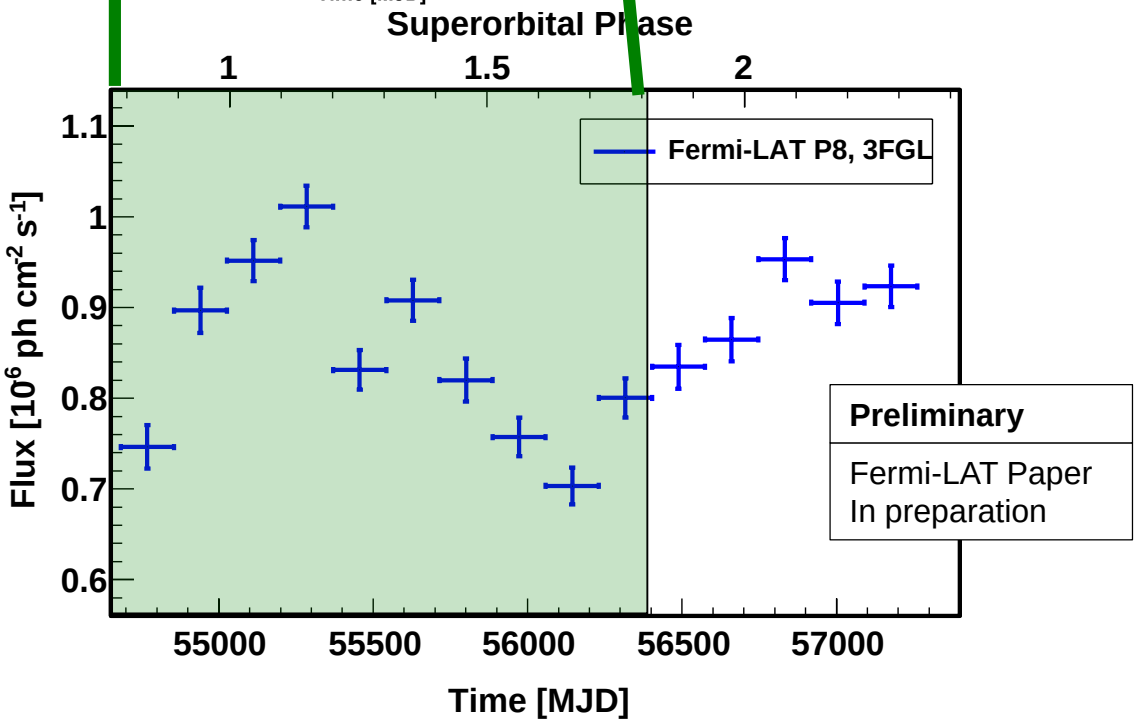

Two short-timescales bursts

Table 1
Bursts Observed by *Swift*-BAT from LS I +61°303

	Burst No. I[a]	Burst No. II[b]
Date	2008 Sep 10	2012 Feb 5
Position uncertainty	2.′1	3′
Angular separation	0.′60	1.′07
T_{100} (s)	0.31	0.044
Fluence (10^{-8} erg cm^{-2})	1.4 ± 0.6	0.58 ± 0.14
Γ	2.0 ± 0.3	3.9 ± 0.4
Luminosity (10^{37} erg s^{-1})	2.1	6.3

Notes. The positional uncertainty is given at a 90% confidence level, including also systematic uncertainties. The angular separation is calculated with respect to the position of the optical counterpart. The T_{100} duration and the fluences are estimated in the 15–50 keV band. Burst spectra were fitted by a power law with index Γ. The average luminosity is estimated by assuming a distance of 2 kpc (Frail & Hjellming 1991).

[a] Torres et al. (2012).

[b] From Burrows et al. (2012); see also http://gcn.gsfc.nasa.gov/notices_s/513505/BA/.

The second burst is essentially the same as the first, but shorter and more luminous

from Papitto, DFT, Rea 2012, ApJ

Focus on LS I +61 303

Flares

- There are no detected pulsations
- But there were two flares, ~0.1 s, with 'high' Lx (orders of magnitude beyond bolometric lum.)
- The bursts were in all aspects similar to SGR ones.
- LS I +61 303 could relate gamma-ray binaries with magnetar systems

[Take into account that magnetar phenomenology is related to the inner magnetic field of neutron stars, not the dipolar: several low-B magnetars are know.]

Table 1
Bursts Observed by *Swift*-BAT from LS I +61°303

	Burst No. I[a]	Burst No. II[b]
Date	2008 Sep 10	2012 Feb 5
Position uncertainty	2.′1	3′
Angular separation	0.′60	1.′07
T_{100} (s)	0.31	0.044
Fluence (10^{-8} erg cm^{-2})	1.4 ± 0.6	0.58 ± 0.14
Γ	2.0 ± 0.3	3.9 ± 0.4
Luminosity (10^{37} erg s^{-1})	2.1	6.3

Notes. The positional uncertainty is given at a 90% confidence level, including also systematic uncertainties. The angular separation is calculated with respect to the position of the optical counterpart. The T_{100} duration and the fluences are estimated in the 15–50 keV band. Burst spectra were fitted by a power law with index Γ. The average luminosity is estimated by assuming a distance of 2 kpc (Frail & Hjellming 1991).

[a] Torres et al. (2012).

[b] From Burrows et al. (2012); see also http://gcn.gsfc.nasa.gov/notices_s/513505/BA/.

DFT, et al. 2012

Super-orbital variability

- Known in radio and Hα (e.g. Gregory 2002)
- Discovered in X-rays after 4+ years of monitoring with RXTE (Li, DFT et el. 2012, Chernyakova et al. 2012)

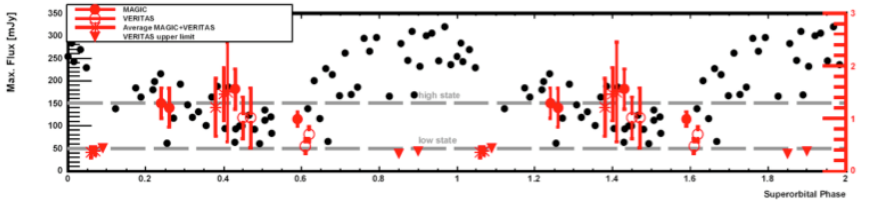

Li, DFT et al. 2012

Variability of lightcurve along the super-orbit

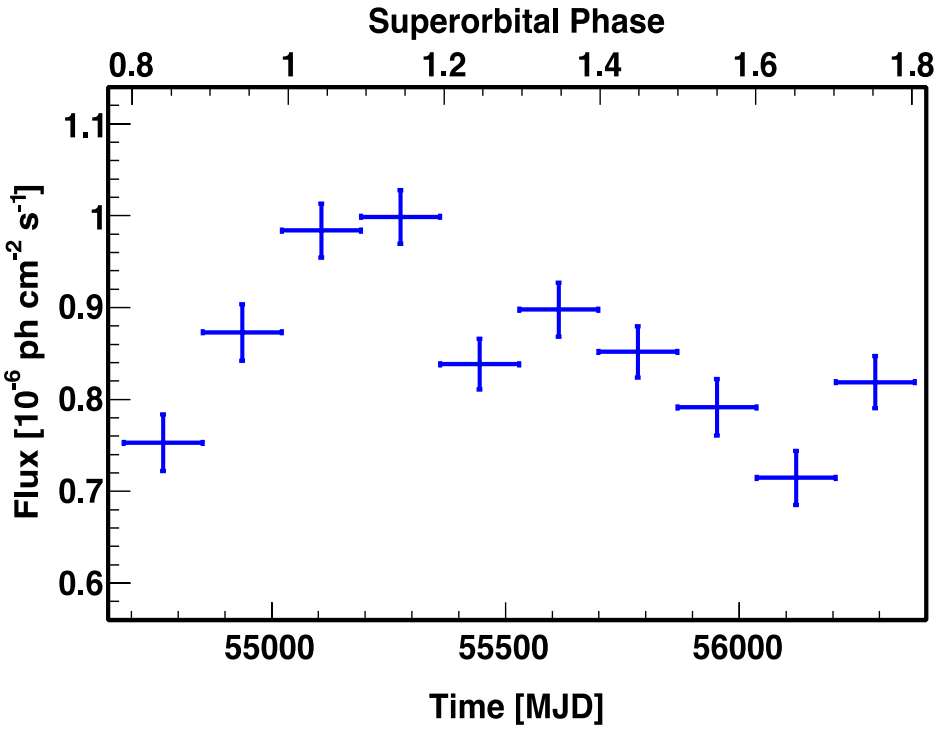

• Best determined superorbital period from radio campaign: (lasting 23 years): 1667±8 days

→Probability that g-ray flux evolution is a random result: $< 1.1 \times 10^{-12}$

→ Source is variable along the superorbit in the GeV regime

Power spectrum analysis (each panel is 169 days of data)

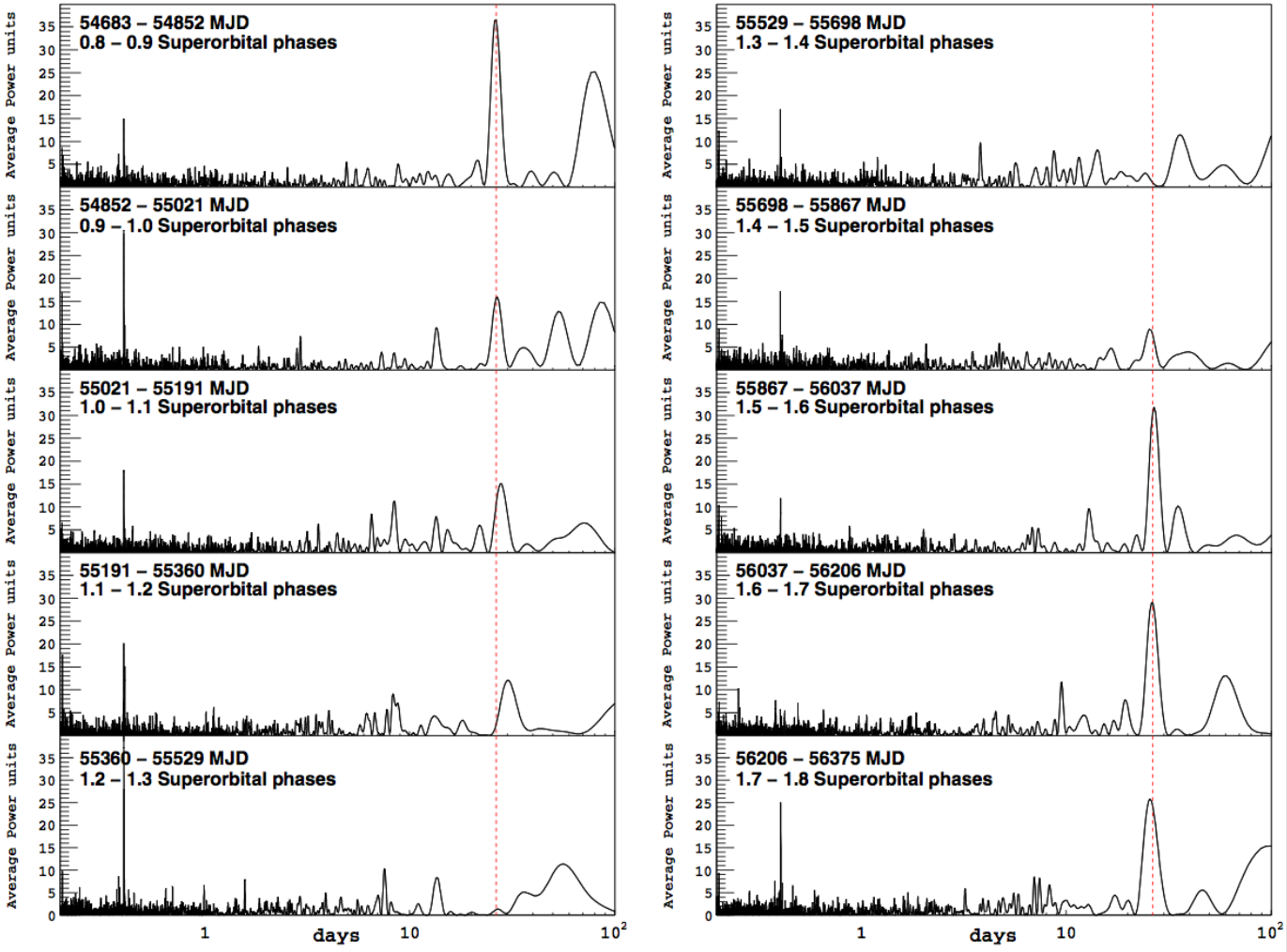

•Slight shift in peaks from nominal period? In the 4th panel it is at 30 days.

→Peaks are within a frequency distance of $1/T_{obs}$ (1/169 days = 0.006) from the nominal frequency 1/26.5 days (0.04). And, they are not significant (all trials probability is low).

3rd power spectrum:

mean = 28.05 +- 0.07 days

width = 1.8 days
Single trial significance = 5.2 sigmas
All trials significance = 3.6 sigmas

4rth power spectrum:
mean = 30.4 +- 0.13 days
width = 2.6 days
Single trial significance = 4.6 sigmas
All trials significance = 2.7 sigmas

Variability in the power

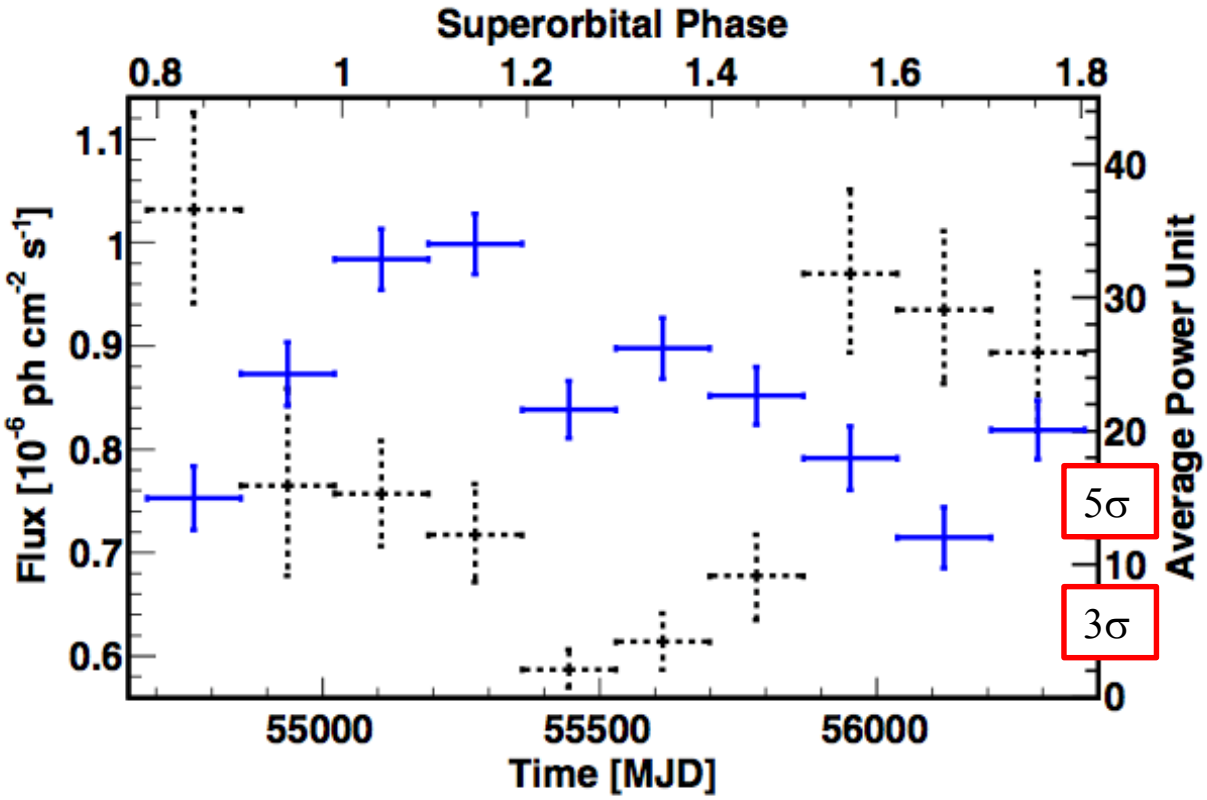

Figure 2. Long-term evolution of the average γ-ray flux (above 100 MeV) from LS I +61°303 (blue points, left *y*-axis scale). The superorbital phase is shown in the top axis. The right *y*-axis scale and the black dashed points show the long-term evolution of the power at the orbital period found in the Lomb–Scargle periodogram.

Can short flares be the result of spectral evolution of longer ones?

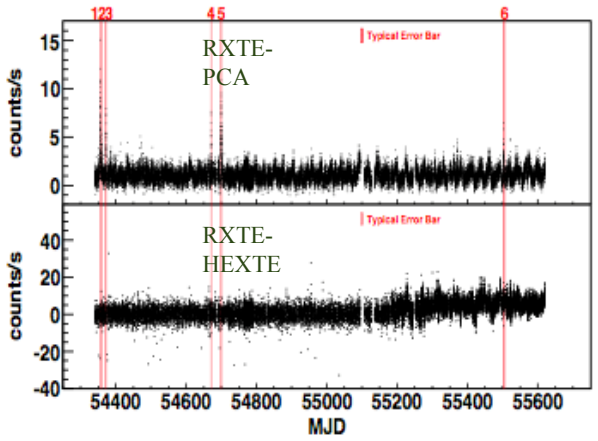

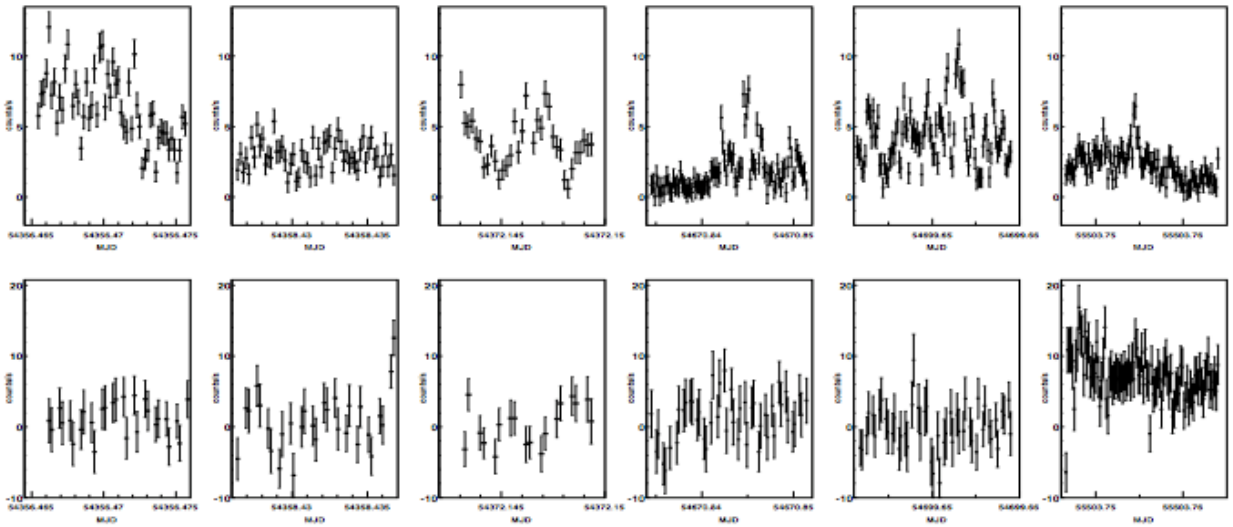

Lightcurve of the 6 flares in 3-10 keV (PCA) as observed at 15–250 keV by HEXTE. All lightcurves are binned at 16 s.

RXTE–HEXTE COUNTERPARTS TO THE SOFT X-RAY FLARES.

Flare	MJD	Average count rate	Significance	reduced χ^2
1	54356	1.057±0.534	0.273	17.49/26
2	54358	0.942±0.520	0.236	64.17/28
3	54372	0.060±0.584	0.048	22.47/17
4	54670	0.975±0.453	0.246	61.40/45
5	54699	-0.008±0.425	0.070	43.20/47
6	55503	6.882±0.279	0.502	133.5/94

NOTE. — The average count rate, significance and reduced χ^2 in the 15–250 keV energy band of the HEXTE data during the ks-timescale flares.

In HEXTE, a Swift-like burst should Have ~5σ

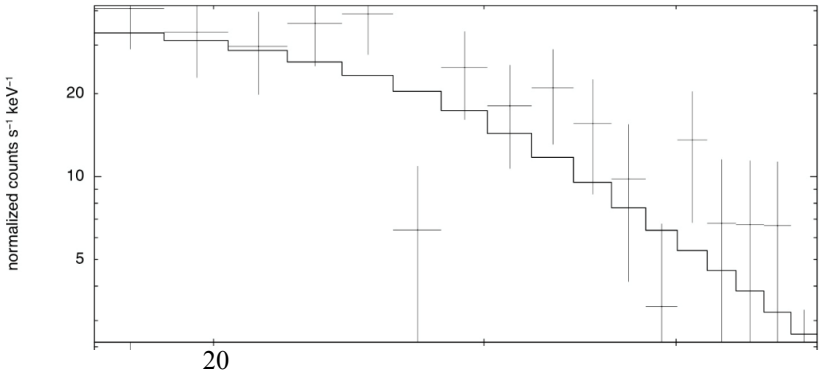

A hard to soft evolution is discarded

Plots from Torres et al. 2011, 2012; both in ApJ

Changes of state in a pulsar binary

Ejector→Propeller→Accretor (and sometimes backwards)

- Interaction with the environment:

Mass within the gravitational capture radius falls towards the NS exerting a pressure

- EM pressure > Matter pressure (at the radius of gravitational capture) for the NS to work as an ejector

- EM pressure ~ $B^2 P^{-4}$
- Matter pressure ~ Mdot

- As the NS decelerates, the matter pressure eventually overcomes the EM pressure and switches the pulsar off

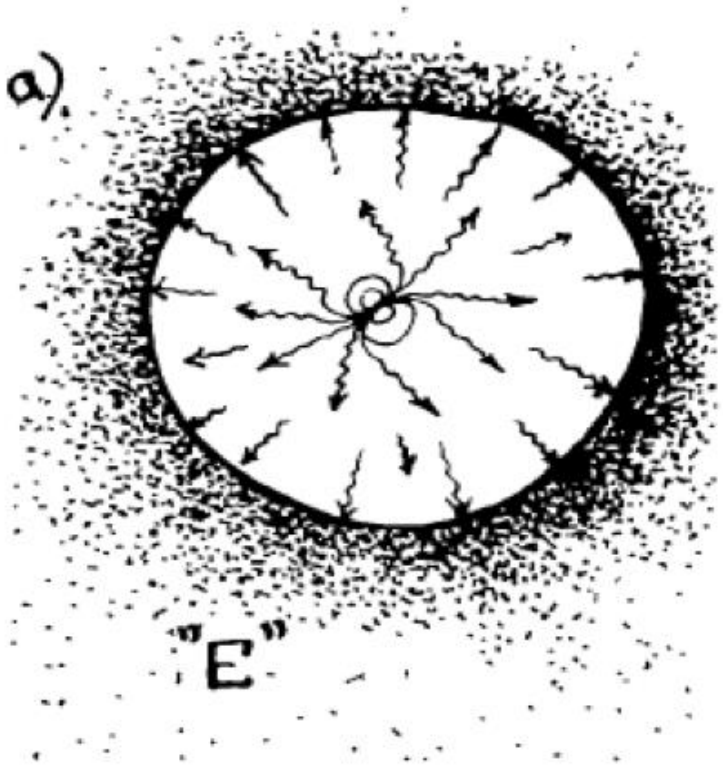

Ideas go back up to Gnusareva & Lipunov 1985

Changes of state in a pulsar binary

Ejector→**Propeller**→Accretor (and sometimes backwards)

- Infalling matter is stopped by the pressure of the magnetosphere
  (Matter pressure = Magnetic pressure)

$$R_M = \frac{(B_1 R_1^3/2)^{4/7}}{\dot{M}^{2/7}(2GM_1)^{1/7}}$$

When $R_M < R_{LC}$ the NS abandons the ejector state

- But since the NS is a fast rotator matter cannot accrete onto the NS

$$R_{co} = \left(\frac{GM_1}{\Omega^2}\right)^{1/3}$$

- Accretion is inhibited as far as $R_M > R_{co}$

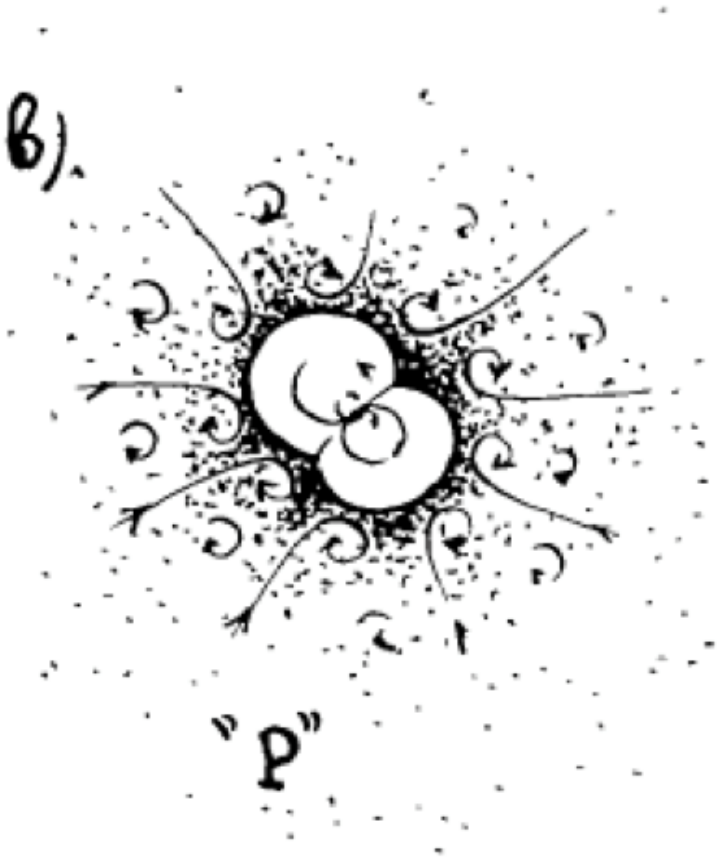

see e.g., Bednarek 2009 for a discussion on the ability of propellers to accelerate particles up to HE

Idea: changes of state in a pulsar binary

Ejector→Propeller→**Accretor** (and sometimes backwards)

Accretion is inhibited as far as energy is released by the rotating NS to the incoming matter at a much larger rate at which the atmosphere can cool down

Only when the NS has slowed down enough that $R_M < R_{CO}$, accretion is allowed, and X-ray pulses should be observed

Flip-flop life is larger than the ejector's

The time it takes for a NS to reach a period P under the action of a spin-down torque $N(P)$ is obtained from the integration of the equation

$$N(P) = I\dot{\Omega} = -\frac{2\pi I}{P^2}\frac{dP}{dt}$$

$$t = -2\pi I \int_{P_0}^{\bar{P}} \frac{dP}{P^2 N(P)}$$

See Papitto, DFT, Rea 2012, ApJ

Flip-flop life is larger than the ejector's

The time it takes for a NS to reach a period P under the action of a spin-down torque $N(P)$ is obtained from the integration of the equation

$$N(P) = I\dot{\Omega} = -\frac{2\pi I}{P^2}\frac{dP}{dt} \qquad t = -2\pi I \int_{P_0}^{\bar{P}} \frac{dP}{P^2 N(P)}$$

Stronger propeller torque (conservative scenario)

Flip – flop timescale:

$$t = 11.7\ \mathrm{kyr}\ (B/5\mathrm{E}13\mathrm{G})^{-1}\ (\dot{M}_{dot}^{max}/5\mathrm{E}16\ \mathrm{g/s})^{-0.3}$$

If the weaker torque is considered, much larger timescales are obtained (168 kyr)

Weak dependence on other parameters

$$t_{ej} / t_{ff} = 0.3\ (B/5\mathrm{E}13\mathrm{G})^{0.24}\ (\dot{M}_{dot}^{max}/5\mathrm{E}16\ \mathrm{g/s})^{-0.28}$$

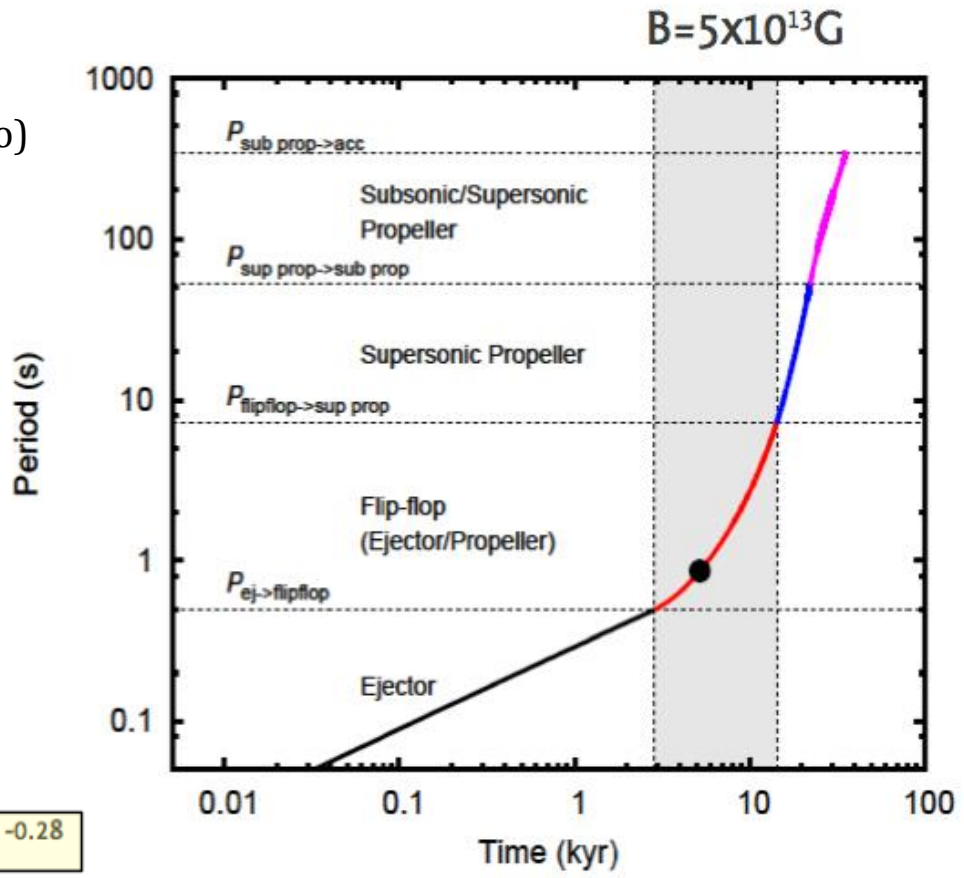

The timescale of flip-flop is larger than that of the ejector

- A NS in an eccentric orbit around a Be star must pass through a flip-flop state.

$$t_{ff} = 11.7\ \mathrm{kyr}\ (B/5E13G)^{-1}\ (M_{dot}^{max}/5E16\ g/s)^{-0.3}$$

$$t_{ej} / t_{ff} = 0.3\ (B/5E13G)^{0.24}\ (M_{dot}^{max}/5E16\ g/s)^{-0.28}$$

- If LS I +61°303 hosts a high field NS which has not yet reached the accretion stage, it is reasonable to find it in the flip-flop state

- Considering the constraint set by the spin down power (>10^{35} erg/s), the system parameters are compatible with a flip-flop timescale of few kyr

  - A mass capture rate at periastron of ~10^{17} g/s (larger by a factor of ~2 than those obtained by sims) is favored by the model

  - To accommodate the superorbital variability in the model, during high radio states the disc should extend throughout the orbit

A magnetar binary, subject to significant changes of accretion around the orbit seems to accommodate observational constraints

See Papitto, DFT, Rea 2012, ApJ

Consider the physical radii (measured from the neutron star)

The light cylinder (the radius at which the magnetic field lines of the neutron star open up):

$$R_{lc} = \frac{cP}{2\pi} \simeq 4.77 \times 10^9 \left(\frac{P}{1\mathrm{s}}\right) \mathrm{cm},$$

The Alfven or magnetic radius is the distance at which the magnetic field starts to dominate the dynamics of the in-falling matter.

$$\frac{B^2}{8\pi} = \frac{1}{2}\rho V_f^2.$$

This simple formula makes use of many things:

$$V_f = \sqrt{\frac{2GM_{ns}}{R}} \qquad B(R) = B_{ns}\left(\frac{R_{ns}}{R}\right)^3 \qquad \rho = \frac{\dot{M}_{acc}}{4\pi R^2 V_f} \qquad \dot{M}_{acc}(r) = \frac{1}{4}\dot{M}_*\left(\frac{R_{cap}}{r}\right)^2 \qquad R_{cap} = \frac{2GM_{ns}}{V_{rel}^2}$$

To define the relative velocity of the neutron star with respect to the accreting matter we need to consider the kind of outflow.

We start by using the polar wind, which is flowing at a velocity of ~1000 km s^{-1}

$$V_w = V_0 + (V_\infty - V_0)\left(1 - \frac{R_*}{r}\right)^\beta \simeq V_\infty\left(1 - \frac{R_*}{r}\right)^\beta$$

and with it, we can compute the radii of interest.

Case of a poloidal wind

Physical radii, and their meaning

$$R_{cap} = \frac{2GM_{ns}}{V_w^2}$$
$$= 3.73 \times 10^{10} \left(\frac{M_{ns}}{1.4M_\odot}\right) \left(\frac{V_\infty}{10^8 \text{ cm s}^{-1}}\right)^{-2}$$
$$\left(1 - 0.69 \left(\frac{R_*}{10R_\odot}\right) \left(\frac{a}{10^{12} \text{ cm}}\right)^{-1}\right.$$
$$\left.(1 - e\cos(\epsilon))^{-1}\right)^{-2\beta} \text{ cm.}$$

$$R_m = 2.1 \times 10^{10} \left(\frac{B}{10^{14}\ G}\right)^{4/7} \left(\frac{\dot{M}_*}{10^{18} \text{ g s}^{-1}}\right)^{-2/7}$$
$$\times \left(\frac{V_\infty}{10^8 \text{ cm s}^{-1}}\right)^{8/7} \left(\frac{a}{10^{12} \text{ cm}}\right)^{4/7}$$
$$\times \left(\frac{R_{ns}}{10^6 \text{ cm}}\right)^{12/7} \left(\frac{M_{ns}}{1.4M_\odot}\right)^{-5/7} (1 - e\cos(\epsilon))^{4/7}$$
$$\times \left(1 - 0.69 \left(\frac{R_*}{10R_\odot}\right) \left(\frac{a}{10^{12} \text{ cm}}\right)^{-1} (1 - e\cos(\epsilon))^{-1}\right)^{8\beta/7} \text{ cm.}$$

$$R_{lc} = \frac{cP}{2\pi} \simeq 4.77 \times 10^9 \left(\frac{P}{1\text{s}}\right) \text{ cm,}$$

The relative comparison between R_m and R_{lc} separates two distinct physical regimes of the system.

When $R_m > R_{lc}$ the magnetosphere of the neutron star remains unscathed by the infalling matter from the stellar wind.

When $R_m < R_{lc}$ matter can continue infalling up to the star surface (direct accretion) or be halted at some distance from the neutron star, within the magnetosphere (e.g., like in a propeller).

The line $R_m = R_{lc}$ thus entails a condition onto P.

Usual magnetar periods are close to defining flip-flop line

In order for the accreting matter to access regions within the magnetosphere,

$$\left(\frac{P}{1\,s}\right) > 4.5 \left(\frac{B}{10^{14}\,G}\right)^{4/7} \left(\frac{\dot{M}_*}{10^{18}\ \mathrm{g\ s^{-1}}}\right)^{-2/7} \times \left(\frac{V_\infty}{10^8\ \mathrm{cm\ s^{-1}}}\right)^{8/7} \left(\frac{a}{10^{12}\ \mathrm{cm}}\right)^{4/7} \times \left(\frac{R_{ns}}{10^6\ \mathrm{cm}}\right)^{12/7} \left(\frac{M_{ns}}{1.4 M_\odot}\right)^{-5/7} (1 - e\cos(\epsilon))^{4/7} \times \left(1 - 0.69 \left(\frac{R_*}{10 R_\odot}\right) \left(\frac{a}{10^{12}\ \mathrm{cm}}\right)^{-1} (1 - e\cos(\epsilon))^{-1}\right)^{8\beta/7}.$$

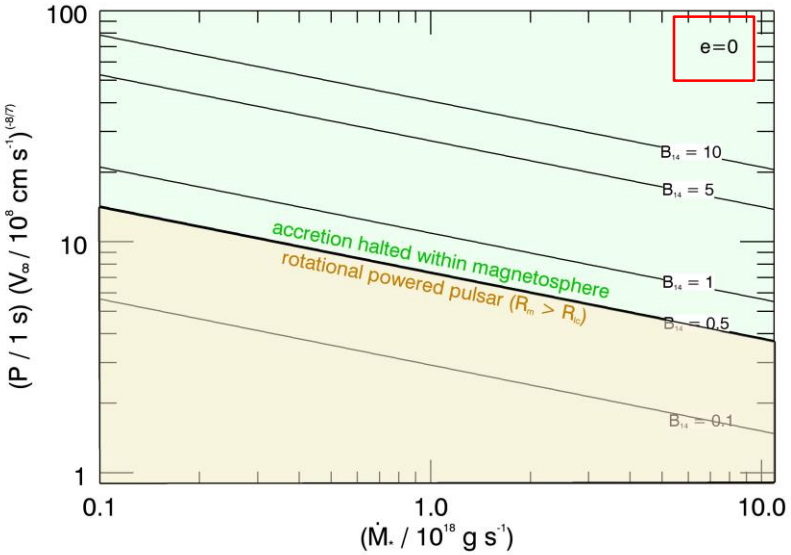

Neutron stars of sufficiently small periods, have an unscathed magnetosphere, and thus behave as a normal pulsar.

Note that the transition between the regimes where the neutron star is accreting within the magnetosphere and that of a rotational powered neutron star happens right at the spin periods usually measured for magnetars.

Plots from DFT, et al. 2012, ApJ

Usual magnetar periods are close to defining flip-flop line

In order for the accreting matter to access regions within the magnetosphere,

$$\left(\frac{P}{1\,s}\right) > 4.5 \left(\frac{B}{10^{14}\,G}\right)^{4/7} \left(\frac{\dot{M}_*}{10^{18}\,\mathrm{g\,s^{-1}}}\right)^{-2/7} \times \left(\frac{V_\infty}{10^{8}\,\mathrm{cm\,s^{-1}}}\right)^{8/7} \left(\frac{a}{10^{12}\,\mathrm{cm}}\right)^{4/7} \times \left(\frac{R_{ns}}{10^{6}\,\mathrm{cm}}\right)^{12/7} \left(\frac{M_{ns}}{1.4 M_\odot}\right)^{-5/7} (1 - e\cos(\epsilon))^{4/7} \times \left(1 - 0.69 \left(\frac{R_*}{10 R_\odot}\right) \left(\frac{a}{10^{12}\,\mathrm{cm}}\right)^{-1} (1 - e\cos(\epsilon))^{-1}\right)^{8\beta/7}.$$

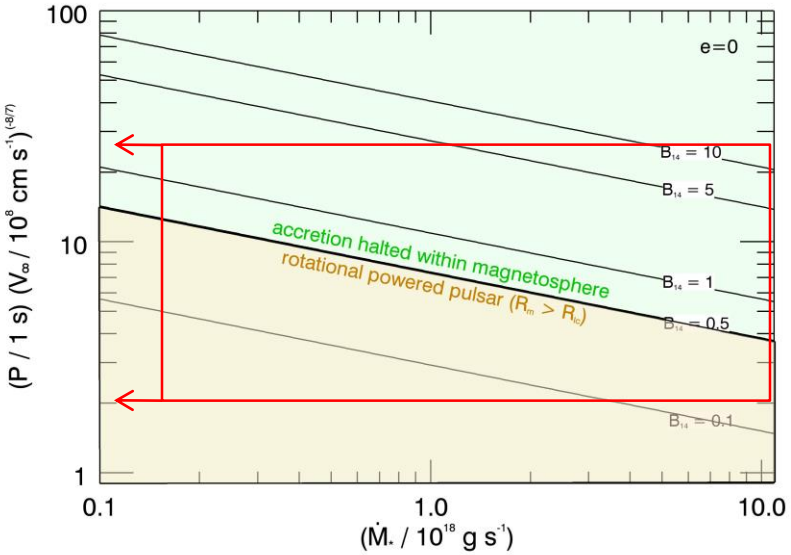

Neutron stars of sufficiently small periods, have an unscathed magnetosphere, and thus behave as a normal pulsar.

note that the transition between the regimes where the neutron star is accreting within the magnetosphere and that of a rotational powered neutron star happens right at the spin periods usually measured for magnetars.

Plots from DFT, et al. 2011

In an eccentric binary system, the conditions over the radii differ

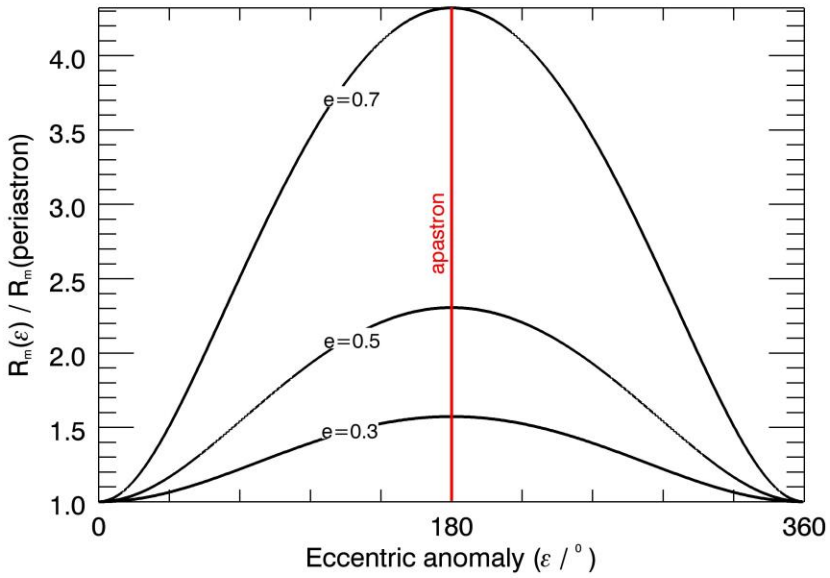

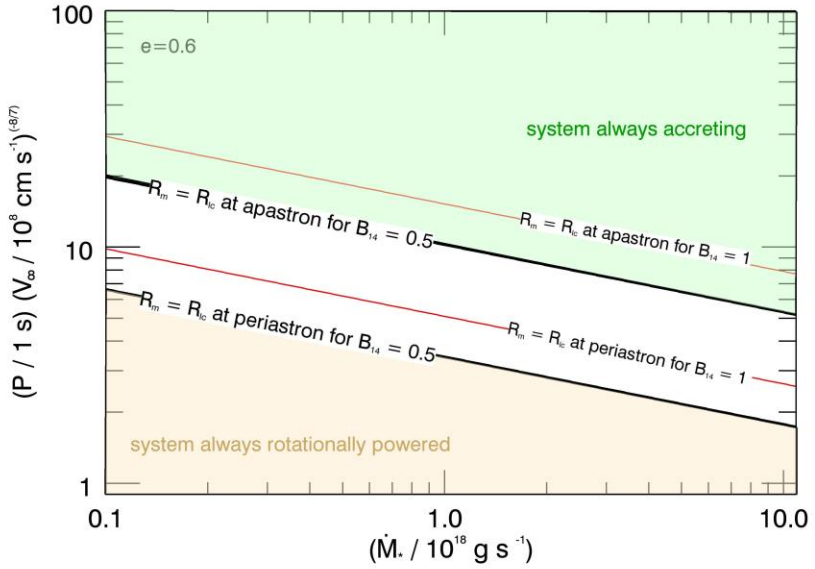

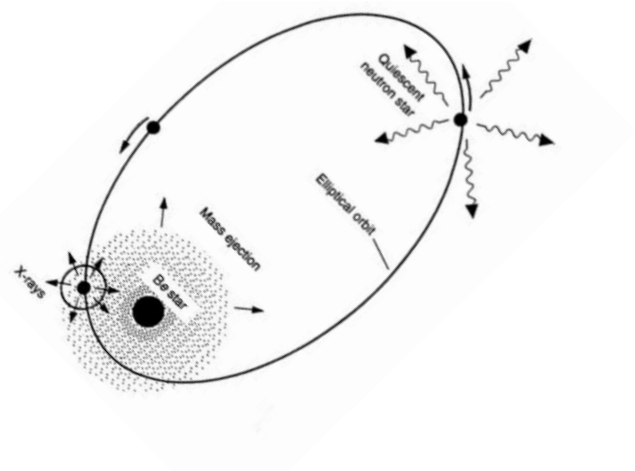

The plots show how much would the magnetospheric radius change because of the orbital motion of the orbit of LS I 61 303; and the regime of flip-flop for different surface magnetic fields.

Plots from DFT, et al. 2012, ApJ

Ejector / propeller torques

$$R_M = \frac{(B_1 R_1^3/2)^{4/7}}{\dot{M}^{2/7}(2GM_1)^{1/7}} \qquad R_{LC} = c/\Omega$$

$R_M > R_{LC}$ ---> Ejector state

$$N_{ej} = -\left(\frac{B_1 R_1^3}{2}\right)^2 \frac{\Omega^3}{c^3}(1+\sin^2\alpha).$$

$R_M < R_{LC}$ ---> Propeller state

- Efficiency of the propeller effect ??? (spherical accretion)
- original Illarionov – Sunyaev (1975)

$$L_{prop}^{(IS)} = \dot{M} v_{ff}^2/2.$$

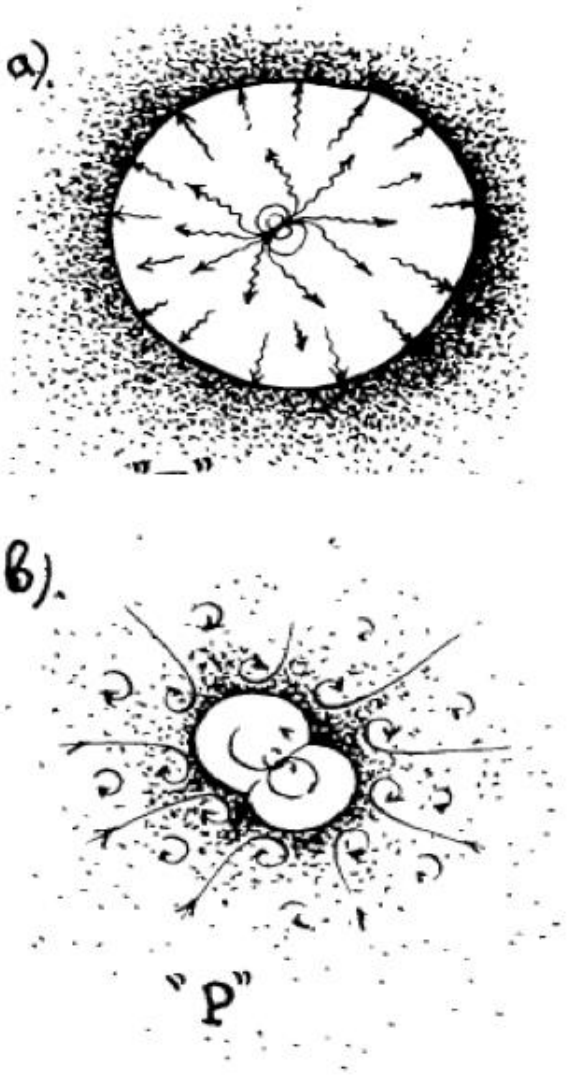

Propeller efficiency

$$N_{\rm prop} = \frac{L_{\rm prop}}{\Omega} \approx \frac{1}{\Omega}\,\epsilon \times 4\pi R_M^2 v_{\rm t}(R_M)$$

No consensus on the value of the energy released during every rotation:

- Davies & Pringle scaling

  $\varepsilon = 1/2\ \rho\ v_{ff}^2$

$$N^{IS}_{prop} = -\dot{M}\sqrt{GM_1R_M}\ \omega_*^{-1}$$

- Mineshige 1991, Ghosh 1995 scaling

  $\varepsilon = 1/2\ \rho\ (\Omega R_M)^2$

$$N^{G}_{prop} = -\frac{1}{6}\dot{M}\sqrt{GM_1R_M}\ \omega_*$$

$\omega = (R_M/R_{co})^{3/2}$ can take values > 100 (!!!)

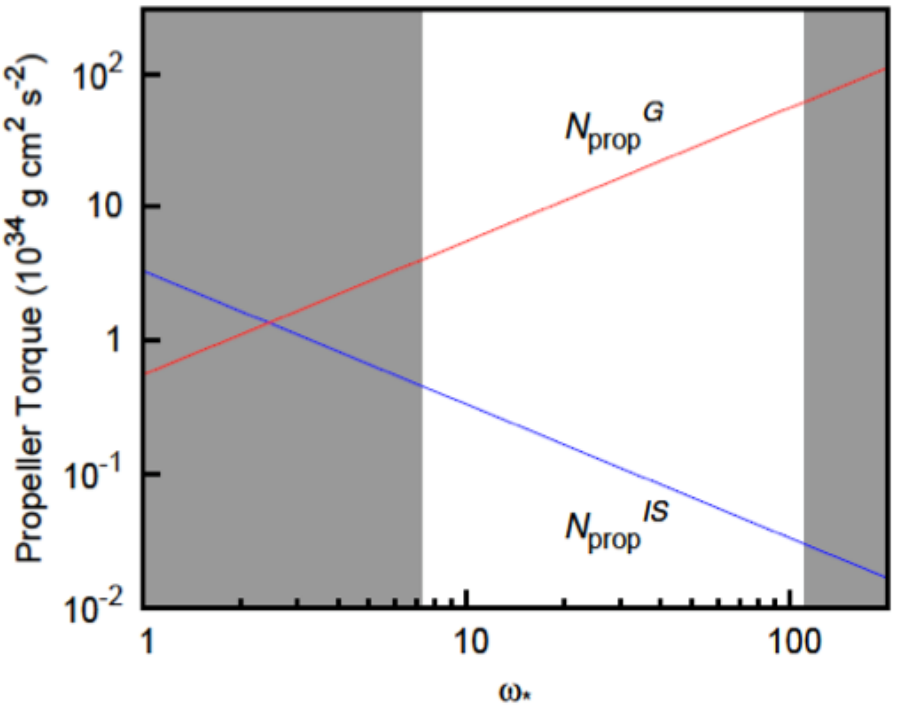

See Papitto, DFT, Rea 2012

Torques

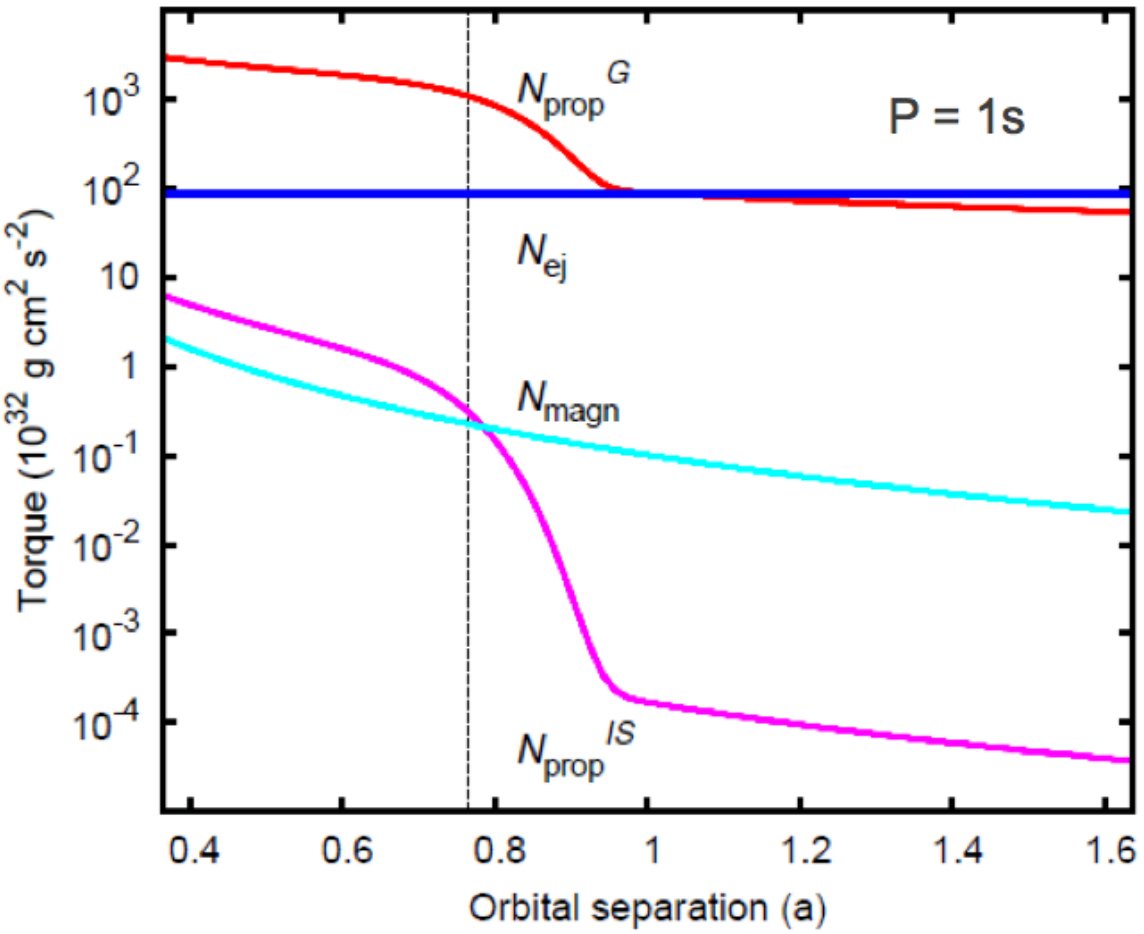

See Papitto, DFT, Rea 2012

Gamma-rays from binaries and gamma-ray binaries

-When gamma-ray emission above 10 MeV 'dominates' the SED output
-Have a distinctive phenomenology in their orbital variability

•This is the case for LS 5039, PSR B1259-63, LS I +61 303, …
•This is not the case of Cyg X-1 (for which $L_{vhe} \sim 10^{-4} L_x$, and was hinted at when flaring only)

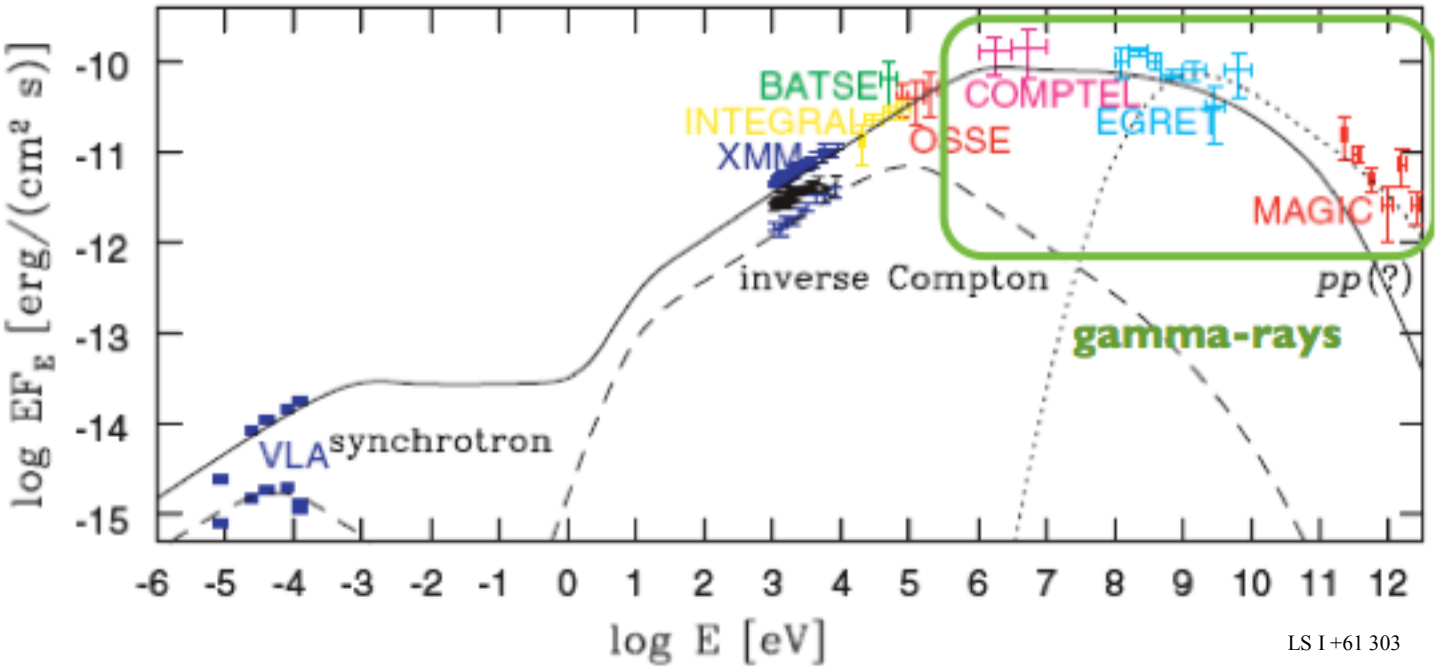

Plot from Chernyakova et al. 2006

Hints of MW inter-relation

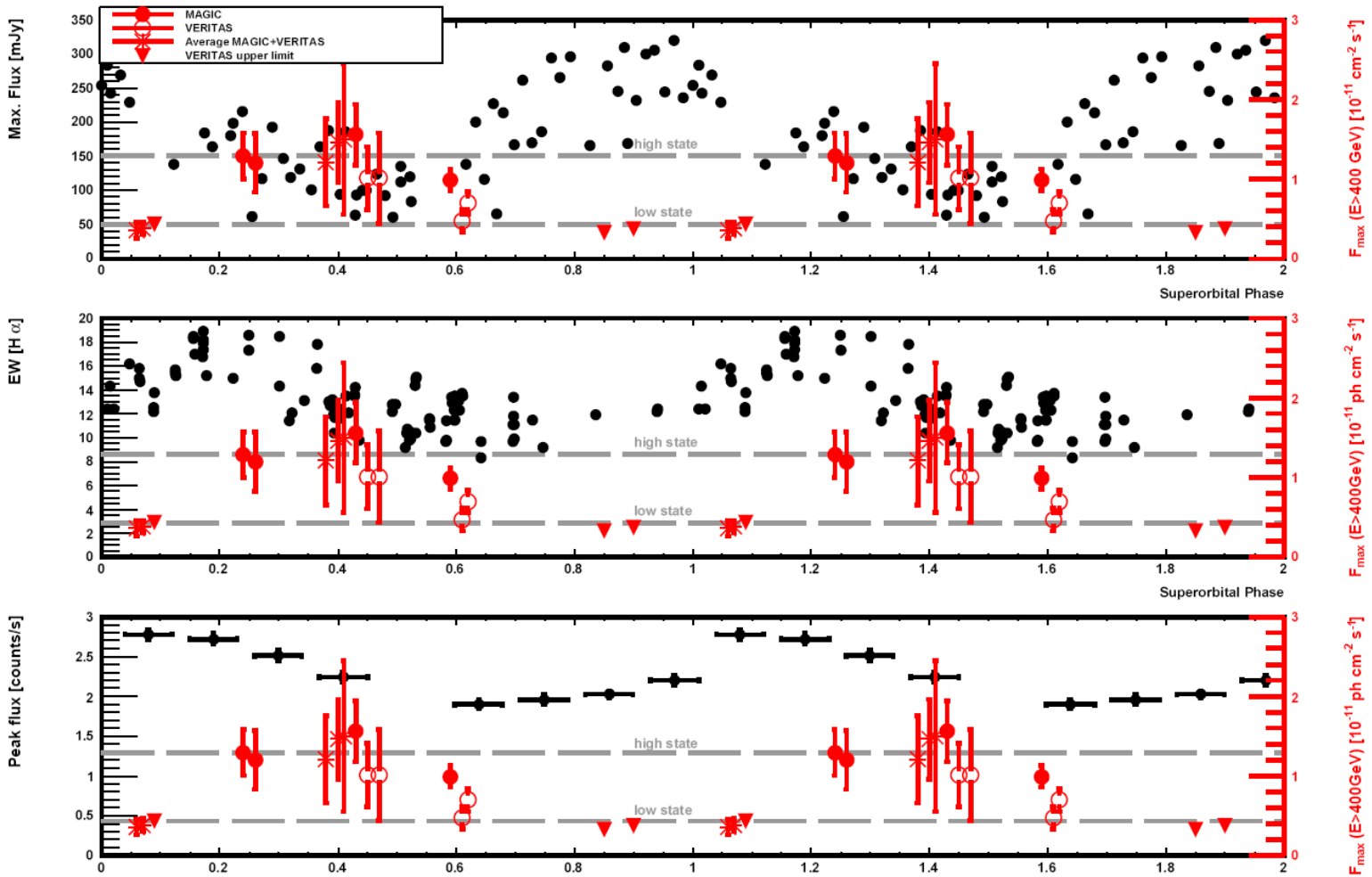

Peak flux per orbit in TeV shown in red (all of them happening in the 0.6–1.0 orbital phase range) as a function of super-orbital phase, together with radio, Hα (black, Zamanov et al. 2000) and X-ray data